PHYSICAL REVIEW D **94,** 094015 (2016)

Direct *CP* violation in charmless three-body decays of *B* mesons

Hai-Yang Cheng,[1] Chun-Khiang Chua,[2] and Zhi-Qing Zhang[3]
[1]*Institute of Physics, Academia Sinica Taipei, Taiwan 115, Republic of China*
[2]*Department of Physics and Center for High Energy Physics, Chung Yuan Christian University, Chung-Li, Taiwan 320, Republic of China*
[3]*Department of Physics, Henan University of Technology, Zhengzhou, Henan 450052, People's Republic of China*
(Received 29 July 2016; published 14 November 2016)

Direct *CP* violation in charmless three-body hadronic decays of *B* mesons is studied within the framework of a simple model based on the factorization approach. Three-body decays of heavy mesons receive both resonant and nonresonant contributions. Dominant nonresonant contributions to tree-dominated and penguin-dominated three-body decays arise from the $b \to u$ tree transition and $b \to s$ penguin transition, respectively. The former can be evaluated in the framework of heavy meson chiral perturbation theory with some modification, while the latter is governed by the matrix element of the scalar density $\langle M_1 M_2 | \bar{q}_1 q_2 | 0 \rangle$. Resonant contributions to three-body decays are treated using the isobar model. Strong phases in this work reside in effective Wilson coefficients, propagators of resonances, and the matrix element of scalar density. In order to accommodate the branching fraction and *CP* asymmetries observed in $B^- \to K^- \pi^+ \pi^-$, the matrix element $\langle K\pi | \bar{s} q | 0 \rangle$ should have an additional strong phase, which might arise from some sort of power corrections such as final-state interactions. We calculate inclusive and regional *CP* asymmetries and find that nonresonant *CP* violation is usually much larger than the resonant one and that the interference effect between resonant and nonresonant components is generally quite significant. If nonresonant contributions are turned off in the $K^+K^-K^-$ mode, the predicted *CP* asymmetries due to resonances will be wrong in sign when confronted with experiment. In our study of $B^- \to \pi^-\pi^+\pi^-$, we find that $\mathcal{A}_{CP}(\rho^0\pi^-)$ should be positive in order to account for *CP* asymmetries observed in this decay. Indeed, both *BABAR* and LHCb measurements of $B^- \to \pi^+\pi^-\pi^-$ indicate positive *CP* asymmetry in the $m(\pi^+\pi^-)$ region peaked at m_ρ. On the other hand, all theories predict a large and negative *CP* violation in $B^- \to \rho^0\pi^-$. Therefore, the issue with *CP* violation in $B^- \to \rho^0\pi^-$ needs to be resolved. Measurements of *CP*-asymmetry Dalitz distributions put very stringent constraints on the theoretical models. We check the magnitude and the sign of *CP* violation in some (large) invariant mass regions to test our model.

DOI: 10.1103/PhysRevD.94.094015

I. INTRODUCTION

The primary goal and the most important mission of *B* factories built before millennium is to search for *CP* violation in the *B* meson system. *BABAR* and Belle Collaborations have measured direct *CP* asymmetries in many two-body charmless hadornic *B* decay channels, but only ten of them have significance larger than 3σ: $B^-/\bar{B}^0 \to K^-\pi^+, \pi^+\pi^-, K^-\eta, \bar{K}^{*0}\eta, K^{*-}\pi^+, K^- f_2(1270), \pi^- f_0(1370), K^-\rho^0, \rho^\pm\pi^\mp$ [1,2], and $B^- \to K^{*-}\pi^0$ [3]. In the B_s system, direct *CP* violation in $\bar{B}_s^0 \to K^+\pi^-$ with 7.2σ significance was measured by LHCb [4]. As for three-body *B* decays, *BABAR* and Belle Collaborations had measured partial rate asymmetries in various charmless three-body modes (see [1,2] or Table I of [5]) and failed to see any evidence.

Recently, LHCb has measured direct *CP* violation in charmless three-body decays of *B* mesons [6–8] and found evidence of inclusive integrated *CP* asymmetries $\mathcal{A}_{CP}^{\rm incl}$ in $B^+ \to \pi^+\pi^+\pi^-$ (4.2σ), $B^+ \to K^+K^+K^-$ (4.3σ), and $B^+ \to K^+K^-\pi^+$ (5.6σ), and a 2.8σ signal of *CP* violation in $B^+ \to K^+\pi^+\pi^-$ (see Table I). Direct *CP* violation in two-body resonances in the Dalitz plot has been seen at *B* factories. For example, both *BABAR* [9] and Belle [10] Collaborations have claimed evidence of partial rate asymmetries in the channel $B^\pm \to \rho^0(770)K^\pm$ in the Dalitz-plot analysis of $B^\pm \to K^\pm\pi^\mp\pi^\pm$. The inclusive *CP* asymmetry in three-body decays results from the interference of the two-body resonances and three-body nonresonant decays and from the tree-penguin interference. *CP* asymmetries in certain local regions of the phase space are likely to be greater than the integrated ones. Indeed, LHCb has also observed large asymmetries in localized regions of phase space (see Table I for $\mathcal{A}_{CP}^{\rm low}$) specified by [6,7]

TABLE I. LHCb results of direct CP asymmetries (in %) for various charmless three-body B^- decays. The superscripts "incl" "low" and "resc"denote CP asymmetries measured in full phase space, in the low invariant mass regions specified in Eq. (1.1) and in the rescattering regions with $1.0 < m_{\pi^+\pi^-,K^+K^-} < 1.5$ GeV, respectively. Data are taken from [6,7] for $\mathcal{A}_{CP}^{\rm low}$ and from [8] for $\mathcal{A}_{CP}^{\rm incl}$ and $\mathcal{A}_{CP}^{\rm resc}$.

	$\pi^+\pi^-\pi^-$	$K^+K^-\pi^-$	$K^-\pi^+\pi^-$	$K^-K^+K^-$
$\mathcal{A}_{CP}^{\rm incl}$	$5.8 \pm 0.8 \pm 0.9 \pm 0.7$	$-12.3 \pm 1.7 \pm 1.2 \pm 0.7$	$2.5 \pm 0.4 \pm 0.4 \pm 0.7$	$-3.6 \pm 0.4 \pm 0.2 \pm 0.7$
$\mathcal{A}_{CP}^{\rm low}$	$58.4 \pm 8.2 \pm 2.7 \pm 0.7$	$-64.8 \pm 7.0 \pm 1.3 \pm 0.7$	$67.8 \pm 7.8 \pm 3.2 \pm 0.7$	$-22.6 \pm 2.0 \pm 0.4 \pm 0.7$
$\mathcal{A}_{CP}^{\rm resc}$	$17.2 \pm 2.1 \pm 1.5 \pm 0.7$	$-32.8 \pm 2.8 \pm 2.9 \pm 0.7$	$12.1 \pm 1.2 \pm 1.7 \pm 0.7$	$-21.1 \pm 1.1 \pm 0.4 \pm 0.7$

$$\begin{aligned}
&\mathcal{A}_{CP}^{\rm low}(K^+K^-K^-), \quad \text{for } m^2_{K^+K^-{\rm high}} < 15\ {\rm GeV}^2, \qquad 1.2 < m^2_{K^+K^-{\rm low}} < 2.0\ {\rm GeV}^2,\\
&\mathcal{A}_{CP}^{\rm low}(K^-\pi^+\pi^-), \quad \text{for } m^2_{K^-\pi^+{\rm high}} < 15\ {\rm GeV}^2, \qquad 0.08 < m^2_{\pi^+\pi^-{\rm low}} < 0.66\ {\rm GeV}^2,\\
&\mathcal{A}_{CP}^{\rm low}(K^+K^-\pi^-), \quad \text{for } m^2_{K^+K^-} < 1.5\ {\rm GeV}^2,\\
&\mathcal{A}_{CP}^{\rm low}(\pi^+\pi^-\pi^-), \quad \text{for } m^2_{\pi^+\pi^-{\rm low}} < 0.4\ {\rm GeV}^2, \qquad m^2_{\pi^+\pi^-{\rm high}} > 15\ {\rm GeV}^2. \qquad (1.1)
\end{aligned}$$

Hence, significant signatures of CP violation were found in the above-mentioned low mass regions devoid of most of the known resonances. LHCb has also studied CP asymmetries in the rescattering regions of $m_{\pi^+\pi^-}$ or $m_{K^+K^-}$ between 1.0 and 1.5 GeV, where the final-state $\pi^+\pi^- \leftrightarrow K^+K^-$ rescattering is supposed to be important in this region. The measured CP asymmetries $\mathcal{A}_{CP}^{\rm resc}$ for the charged final states are given in Table I.

In two-body B decays, the measured CP violation is just a number. But in three-body decays, one can measure the distribution of CP asymmetry in the Dalitz plot. Hence, the Dalitz-plot analysis of $\mathcal{A}_{CP}$ distributions can reveal very rich information about CP violation. Besides the integrated CP asymmetry, local asymmetry can be very large and positive in some region and becomes very negative in the other region. The sign of CP asymmetries varies from region to region. A successful model must explain not only the inclusive asymmetry but also regional CP violation. Therefore, the study of three-body CP-asymmetry Dalitz distributions provides a great challenge to the theorists. LHCb has measured the raw asymmetry $A_{\rm raw}$ distributions in the Dalitz plots defined by [8]

$$A_{\rm raw} = \frac{N_{B^-} - N_{B^+}}{N_{B^-} + N_{B^+}} \qquad (1.2)$$

in terms of numbers of B^- and B^+ signal events N_{B^-} and N_{B^+}, respectively. The relation between $A_{\rm raw}$ and $\mathcal{A}_{CP}$ is given in [6–8]. Two-body invariant-mass projection plots are available in Figs. 4–7 of [8]. For CP Dalitz asymmetries in high invariant mass regions, see [11].

Three-body decays of heavy mesons are more complicated than the two-body case as they receive both resonant and nonresonant contributions. The analysis of these decays using the Dalitz plot technique enables one to study the properties of various vector and scalar resonances. Indeed, most of the quasi-two-body decays are extracted from the Dalitz-plot analysis of three-body ones. In this work, we shall focus on charmless B decays into three pseudoscalar mesons.

Contrary to three-body D decays, where the nonresonant signal is usually rather small and less than 10% [1], nonresonant contributions play an essential role in penguin-dominated three-body B decays. For example, the nonresonant fraction of KKK modes is of order 70%–90%. It follows that nonresonant contributions to the penguin-dominated modes should be also dominated by the penguin mechanism. It has been shown in [5,12] that large nonresonant signals arise mainly from the penguin amplitude governed by the matrix element of scalar densities $\langle M_1 M_2|\bar{q}_1 q_2|0\rangle$. We use the measurements of $\bar{B}^0 \to K_S K_S K_S$ to constrain the nonresonant component of $\langle K\bar{K}|\bar{s}s|0\rangle$ [12].

Even for tree-dominated three-body decays such as $B^- \to \pi^-\pi^+\pi^-$, the nonresonant fraction is about 35%. In this case, dominant nonresonant contributions arise from the $b \to u$ tree transition, which can be evaluated using heavy meson chiral perturbation theory (HMChPT) [13–15] valid in the soft meson limit. The momentum dependence of nonresonant $b \to u$ transition amplitudes is parametrized in an exponential form $e^{-\alpha_{\rm NR} p_B\cdot(p_i+p_j)}$ so that the HMChPT results are recovered in the soft meson limit where p_i, $p_j \to 0$. The parameter $\alpha_{\rm NR}$ is fixed by the measured nonresonant rate in $B^- \to \pi^+\pi^-\pi^-$.

Besides the nonresonant background, it is necessary to study resonant contributions to three-body decays. Resonant effects are conventionally described using the isobar model in terms of the usual Breit-Wigner formalism. In this manner we are able to identify the relevant resonances which contribute to the three-body decays of interest and compute the rates of $B \to VP$ and $B \to SP$, where the intermediate vector meson contributions to three-body decays are identified through the vector current, while the scalar meson resonances are mainly associated with the

scalar density. They can also contribute to the three-body matrix element $\langle P_1P_2|J_\mu|B\rangle$.

The recent LHCb measurements of integrated and local direct CP asymmetries in charmless $B \to P_1P_2P_3$ decays (see Table I) provide a new insight of the underlying mechanism of three-body decays. The observed negative relative sign of CP asymmetries between $B^- \to \pi^-\pi^+\pi^-$ and $B^- \to K^-K^+K^-$ and between $B^- \to K^-\pi^+\pi^-$ and $B^- \to \pi^-K^+K^-$ is in accordance with what expected from U-spin symmetry which enables us to relate the $\Delta S = 0$ amplitude to the $\Delta S = 1$ one. However, symmetry arguments alone do not tell us the relative sign of CP asymmetries between $\pi^-\pi^+\pi^-$ and $\pi^-K^+K^-$ and between $K^-\pi^+\pi^-$ and $K^-K^+K^-$. The observed asymmetries (integrated or regional) by LHCb are positive for $h^-\pi^+\pi^-$ and negative for $h^-K^+K^-$ with $h = \pi$ or K. The former usually has a larger CP asymmetry in magnitude than the latter. This has led to the conjecture that $\pi^+\pi^- \leftrightarrow K^+K^-$ rescattering may play an important role in the generation of the strong phase difference needed for such a violation to occur [8].

After the LHCb measurement of direct CP violation in three-body charged B decays, there are some theoretical works in this regard [5,16–27]. In the literature, almost all the works focus on resonant contributions to the rates and asymmetries. This is understandable in terms of the experimental observation that 90% of the Dalitz plot events has $m(h^+h^-)^2 < 3.0\ \mathrm{GeV}^2$ [28]. The events are concentrated in low-mass regions, implying the dominance of charmless decays by resonant contributions. Nevertheless, in [5], we have examined CP violation in three-body decays and stressed the crucial role played by the nonresonant contributions. Indeed, if the nonresonant term is essential to account for the total rate, it should play some role to CP violation. In this work, we would like to study asymmetries arising from both resonant and nonresonant amplitudes and their interference. This will make it clear the relative weight of both contributions and their interference.

It has been argued in [24] that the amplitude at the Dalitz plot center is expected to be both power and strong coupling α_s suppressed with respect to the amplitude at the edge. The perturbative regime in the central region gets considerably reduced for realistic value of m_B. That is, the Dalitz plot is completely dominated by the edges. Since the nonresonant background arises not just from the central region, the above argument is not inconsistent with the experimental observation of dominant nonresonant signals in penguin-dominated three-body decays.

There are several competing approaches for describing charmless hadronic two-body decays of B mesons, such as QCD factorization (QCDF) [29], perturbative QCD (pQCD) [30], and soft-collinear effective theory (SCET) [31]. Unlike the two-body case, to date we still do not have theories for hadronic three-body decays, though attempts along the framework of pQCD and QCDF have been made in the past [22,24,32]. In this work, we shall take the factorization approximation as a working hypothesis rather than a first-principles starting point as factorization has not been proven for three-body B decays. That is, we shall work in the phenomenological factorization model rather than in the established QCD-inspired theories.

The layout of the present paper is as follows. In Sec. II, we discuss resonant and nonresonant contributions to three-body B decays. The predicted rates for penguin-dominated $B \to VP$ modes are generally too small compared to experiment. We add power corrections induced by penguin annihilation to these modes to render a better agreement with the data. Section III is devoted to direct CP violation. We consider inclusive and regional CP asymmetries arising from both resonant and nonresonant mechanisms. The effect of final-state rescattering is discussed. Comparison of our work with others available in the literature is made in Sec. IV. Section V contains our conclusions.

II. THREE-BODY DECAYS

Many three-body B decays have been observed with branching fractions of order 10^{-5} for penguin-dominated $B \to K\pi\pi, KKK$ decays, and of order 10^{-6} for tree-dominated $B \to \pi\pi\pi, K\pi\pi$. The charmless three-body channels that have been measured are [1]

$$\begin{aligned}
&B^- \to \pi^+\pi^-\pi^-, && K^-\pi^+\pi^-, && \bar{K}^0\pi^-\pi^0, && K^+K^-\pi^-,\\
&\quad K^+K^-K^-, && K^-\pi^0\pi^0, && K^-K_SK_S, && K_S\pi^-\pi^0,\\
&\bar{B}^0 \to \pi^+\pi^-\pi^0, && \bar{K}^0\pi^+\pi^-, && K^-\pi^+\pi^0, && K^+K^-\pi^0,\\
&\quad K^0K^-\pi^+, && \bar{K}^0K^+\pi^-, && K^+K^-\bar{K}^0, && K_SK_SK_S,\\
&\bar{B}_s^0 \to K^0\pi^+\pi^-, && K^0K^+K^-, && \bar{K}^0K^-\pi^+, && K^0K^+\pi^-.
\end{aligned} \tag{2.1}$$

In B^- and $\bar{B}^0$ three-body decays, the $b \to sq\bar{q}$ penguin transitions contribute to the final states with odd number of kaons, namely, KKK and $K\pi\pi$, while $b \to uq\bar{q}$ tree and $b \to dq\bar{q}$ penguin transitions contribute to final states with even number of kaons, e.g., $KK\pi$ and $\pi\pi\pi$. For $\bar{B}_s^0$ three-body decays, the situation is the other way around.

Consider the three-body decays $B \to P_1P_2P_3$. The b quark decays into three energetic quarks, $q_1q_2\bar{q}_3$. There exist four possible physical configurations depicted in Fig. 1: (a) all three produced mesons are moving energetically, (b) two of the energetic mesons, say P_1 and P_2, are moving collinearly to each other, (c) P_3 is formed from $q_1\bar{q}_3$ or $q_2\bar{q}_3$, while P_2 contains the spectator quark which becomes hard after being kicked by a hard gluon, and (d) is the same as (c) except that P_2 is soft. Configurations (b) and (c) mimic quasi-two-body decays. In the Dalitz plot of Fig. 2, configuration (a) appears in the central region, while configurations (b)–(d) manifest along the edges of

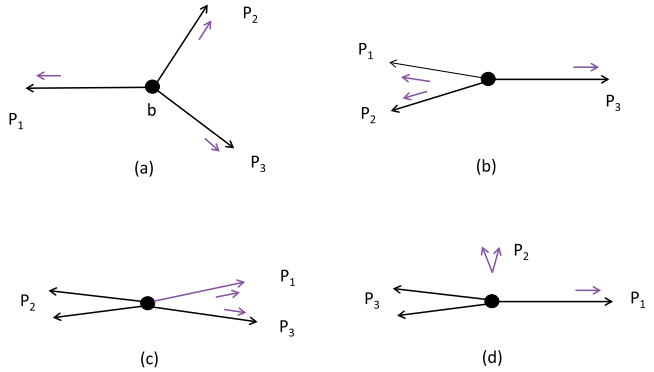

FIG. 1. Possible configurations of three-body $B \to P_1P_2P_3$ decays, where the black lines with arrows denote the momenta of the three energetic quarks $q_1q_2\bar{q}_3$ produced in the b-quark decay, and the pink lines with arrows denote the momenta of the spectator quark and the quark-antiquark pair: (a) all three produced mesons are moving energetically, (b) two of the energetic mesons, say P_1 and P_2, are moving collinearly to each other, recoiling against P_3, (c) P_2 is formed from $q_1\bar{q}_3$ or $q_2\bar{q}_3$, while P_1 contains the spectator quark (denoted by the longer pink line), which becomes hard after being kicked by a hard gluon, and (d) is similar to (c) except that P_2 is soft.

the Dalitz plot. The two mesons P_1 and P_2 in (b) move collinearly, recoiling against P_3. Hence, the invariant mass squared m_{12}^2 is minimal, while the momentum p_3 of P_3 is maximal. Likewise, configuration (c) has minimal m_{13}^2. Resonances show up in configurations (b) and (c), corresponding to quasi-two-particle decays. Therefore, the Dalitz plot for three-body B decays can be divided into several subregions with distinct kinematics and factorization properties, which have been investigated in [24]. Especially, the regions containing the configuration (b) or (c) can be described in terms of two-meson distribution amplitudes and $B \to P_1P_2$ form factors [33–35].

With the advent of heavy quark effective theory, nonleptonic B decays can be analyzed systematically within the QCD framework. There are three popular approaches available in this regard: QCDF, pQCD, and SCET. Theories of hadronic B decays are based on the "factorization theorem" under which the short-distance contributions to the decay amplitudes can be separated from the process-independent long-distance parts. In the QCDF approach, nonfactorizable contributions to the hadronic matrix elements can be absorbed into the effective parameters a_i

$$A(B \to M_1M_2) = \frac{G_F}{\sqrt{2}} \sum \lambda_i a_i(M_1M_2) \langle M_1M_2|O_i|B\rangle_{\rm fact}, \tag{2.2}$$

where a_i are basically the Wilson coefficients in conjunction with short-distance nonfactorizable corrections such as vertex, penguin corrections, and hard spectator interactions, and $\langle M_1M_2|O_i|B\rangle_{\rm fact}$ is the matrix element evaluated under the factorization approximation. Since power corrections of order $\Lambda_{\rm QCD}/m_b$ are suppressed in the heavy quark limit, nonfactorizable corrections to nonleptonic decays are calculable. In the limits of $m_b \to \infty$ and $\alpha_s \to 0$, naive factorization is recovered in both QCDF and pQCD approaches.

Unlike hadronic two-body B decays, established theories such as QCDF, pQCD, and SCET are still not available for three-body decays, though attempts along the framework of pQCD and QCDF have been made in the past [22,24,32]. This is mainly because the aforementioned factorization theorem has not been proven for three-body decays. Hence, we follow [5,12] to take the factorization approximation as a working hypothesis rather than a first-principles starting point.

One of the salient features of three-body B decays is the large nonresonant fraction in penguin-dominated B decay modes, recalling that the nonresonant signal in charm decays is very small, less than 10% [1]. Many of the charmless B to three-body decay modes have been measured at B factories and studied using the Dalitz-plot analysis. The measured fractions and the corresponding

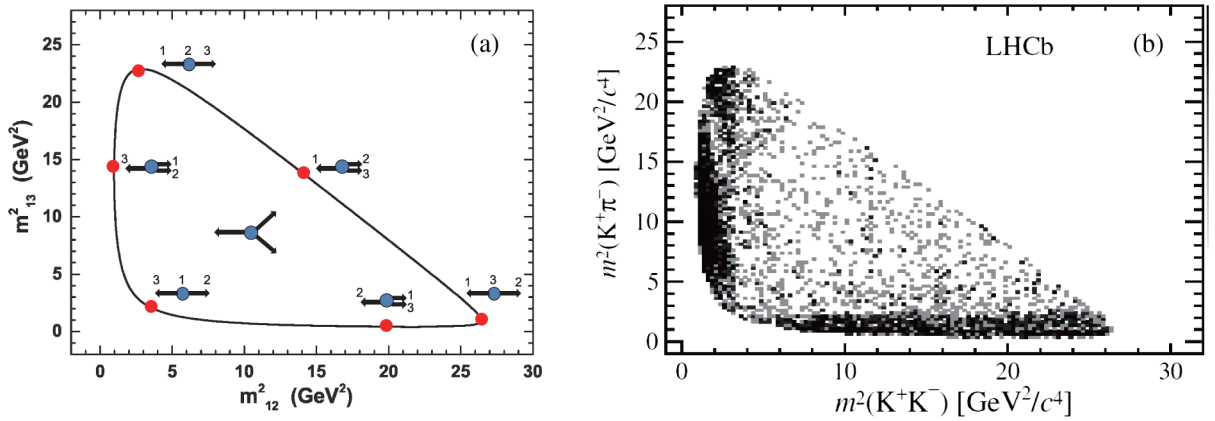

FIG. 2. (a) Location of various physical configurations depicted in Fig. 1 within the Dalitz plot of $B^- \to K^+(p_1)K^-(p_2)\pi^-(p_3)$ and (b) the measured Dalitz plot distribution taken from [8].

TABLE II. The fractions and branching fractions of nonresonant components of various charmless three-body decays of B mesons.

	BABAR		Belle		
Decay	$\mathcal{B}_{\rm NR}(10^{-6})$	NR fraction(%)	$\mathcal{B}_{\rm NR}(10^{-6})$	NR fraction(%)	Reference
$B^- \to K^+K^-K^-$	$22.8 \pm 2.7 \pm 7.6$	$68.3 \pm 8.1 \pm 22.8$	$24.0 \pm 1.5 \pm 1.5$	$78.4 \pm 5.8 \pm 7.7$	[36,37]
$B^- \to K^-K_SK_S$	$19.8 \pm 3.7 \pm 2.5$	~ 196			[36]
$\bar{B}^0 \to K^+K^-\bar{K}^0$	$33 \pm 5 \pm 9$	~ 130			[36]
$\bar{B}^0 \to K_SK_SK_S$	$13.3^{+2.2}_{-2.3} \pm 2.2$	~ 215			[38]
$B^- \to K^-\pi^+\pi^-$	$9.3 \pm 1.0^{+6.9}_{-1.7}$	$17.1 \pm 1.7^{+12.4}_{-1.8}$	$16.9 \pm 1.3^{+1.7}_{-1.6}$	$34.0 \pm 2.2^{+2.1}_{-1.8}$	[9,10]
$\bar{B}^0 \to \bar{K}^0\pi^+\pi^-$	$11.1^{+2.5}_{-1.0} \pm 0.9$	$22.1^{+2.8}_{-2.0} \pm 2.2$	$19.9 \pm 2.5^{+1.7}_{-2.0}$	$41.9 \pm 5.1^{+1.5}_{-2.6}$	[39,40]
$\bar{B}^0 \to K^-\pi^+\pi^0$	$7.6 \pm 0.5 \pm 1.0$	$19.7 \pm 1.4 \pm 3.3$	$5.7^{+2.7+0.5}_{-2.5-0.4}$	< 25.7	[41,42]
$B^- \to \pi^+\pi^-\pi^-$	$5.3 \pm 0.7^{+1.3}_{-0.8}$	$34.9 \pm 4.2^{+8.0}_{-4.5}$			[43]

branching fractions of nonresonant components are summarized in Table II. We see that the nonresonant fraction is about ∼70%–90% in $B \to KKK$ decays, ∼17%–40% in $B \to K\pi\pi$ decays, and ∼35% in the $B \to \pi\pi\pi$ decay. Moreover, we have the hierarchy pattern

$$\mathcal{B}(B \to KKK)_{\rm NR} > \mathcal{B}(B \to K\pi\pi)_{\rm NR} > \mathcal{B}(B \to \pi\pi\pi)_{\rm NR}. \tag{2.3}$$

Hence, the nonresonant contributions play an essential role in penguin-dominated B decays. This is not unexpected because the energy release scale in weak B decays is of order 5 GeV, whereas the major resonances lie in the energy region of 0.77 to 1.6 GeV. Consequently, it is likely that three-body B decays will receive sizable nonresonant contributions. It is important to understand and identify the underlying mechanism for nonresonant decays.

It has been argued in [24] that the Dalitz plot is completely dominated by the edges as the amplitude at the center is both power and α_s suppressed with respect to the one at the edge. As a result, three-body decays become quasi two-body ones. Nevertheless, this argument is not inconsistent with the experimental observation of dominant nonresonant background in penguin-dominated three-body decays because the nonresonant background exists in the whole phase space. That is, the vast phase space of charmless three-body B decays is populated by nonresonant components.

The explicit expressions of factorizable amplitudes of charmless $B \to P_1P_2P_3$ decays can be found in [5,12]. There are three distinct factorizable terms: (i) the current-induced process with a meson emission, $\langle B \to P_1\rangle \times \langle 0 \to P_2P_3\rangle$, (ii) the transition process, $\langle B \to P_1P_2\rangle \times \langle 0 \to P_3\rangle$, and (iii) the annihilation process $\langle B \to 0\rangle \times \langle 0 \to P_1P_2P_3\rangle$, where $\langle A \to B\rangle$ denotes a $A \to B$ transition matrix element. There are two different kinds of mechanisms for the production of a meson pair. In $\langle 0 \to P_2P_3\rangle$, the meson pair is produced from the vacuum through a current, whereas in $\langle B \to P_1P_2\rangle$, the meson pair is produced through a current that induces the transition from the B meson. Hence, we call these as current-induced and transition mechanisms, respectively.[1] While the latter process is produced at the $b \to u$ tree level, the former one is induced at the $b \to s$ or $b \to d$ penguin level. Schematically, the decay amplitude is the coherent sum of resonant contributions together with the nonresonant background

$$A = \sum_R A_R + A_{\rm NR}. \tag{2.4}$$

In the following, we will discuss these two contributions separately.

A. Nonresonant background

Consider the transition process induced by the $b \to u$ current. The nonresonant contribution to the three-body matrix element $\langle P_1P_2|(\bar{u}b)_{V-A}|B\rangle$ has the general expression [44]

$$\begin{aligned}&\langle P_1(p_1)P_2(p_2)|(\bar{u}b)_{V-A}|B\rangle^{\rm NR}\\ &= ir(p_B - p_1 - p_2)_\mu + i\omega_+(p_2 + p_1)_\mu + i\omega_-(p_2 - p_1)_\mu\\ &\quad + h\epsilon_{\mu\nu\alpha\beta}p_B^\nu(p_2 + p_1)^\alpha(p_2 - p_1)^\beta,\end{aligned} \tag{2.5}$$

where $(\bar{q}_1q_2)_{V-A} = \bar{q}_1\gamma_\mu(1-\gamma_5)q_2$. The form factors r, $\omega_\pm$, and h can be evaluated in the framework of heavy meson chiral perturbation theory (HMChPT) [44]. Consequently, the nonresonant amplitude induced by the transition process reads

$$\begin{aligned}&A^{\rm HMChPT}_{\rm transition}\\ &\equiv \langle P_3(p_3)|(\bar{q}u)_{V-A}|0\rangle\langle P_1(p_1)P_2(p_2)|(\bar{u}b)_{V-A}|B\rangle^{\rm NR}\\ &= -\frac{f_{P_3}}{2}[2m_3^2 r + (m_B^2 - s_{12} - m_3^2)\omega_+\\ &\quad + (s_{23} - s_{13} - m_2^2 + m_1^2)\omega_-].\end{aligned} \tag{2.6}$$

[1]Note that the terminology concerning current-induced and transition mechanisms in this work is different to those in our previous publications [5,12].

However, as pointed out in [5,12], the predicted nonresonant rates based on HMChPT are unexpectedly too large for tree-dominated decays. For example, the branching fractions of nonresonant $B^- \to \pi^+\pi^-\pi^-$ and $B^- \to K^+K^-\pi^-$ are found to be of order 75×10^{-6} and 33×10^{-6}, respectively, which are one order of magnitude larger than the corresponding measured total branching fractions of 15.2×10^{-6} and 5.0×10^{-6} (see Table III below). The issue has to do with the applicability of HMChPT. In order to apply this approach, two of the final-state pseudoscalars in $B \to P_1P_2$ transition have to be soft; their momenta should be smaller than the chiral symmetry breaking scale of order 1 GeV. Therefore, it is not justified to apply chiral and heavy quark symmetries to a certain kinematic region and then generalize it to the region beyond its validity. Following [12], we shall assume the momentum dependence of nonresonant amplitudes in an exponential form, namely,

$$A_{\rm transition} = A^{\rm HMChPT}_{\rm transition} e^{-\alpha_{\rm NR} p_B\cdot(p_1+p_2)} e^{i\phi_{12}}, \qquad (2.7)$$

so that the HMChPT results are recovered in the soft meson limit of $p_1,\ p_2 \to 0$. This is similar to the empirical

TABLE III. Branching fractions (in units of 10^{-6}) of resonant and nonresonant (NR) contributions to $B^- \to \pi^-\pi^+\pi^-$, $K^-\pi^+\pi^-$, $K^+K^-\pi^-$, $K^+K^-K^-$. Note that the *BABAR* result for $K_0^{*0}(1430)\pi^-$ in [9] is their absolute one. We have converted them into the product branching fractions, namely, $\mathcal{B}(B \to Rh) \times \mathcal{B}(R \to hh)$. The nonresonant background in $B^- \to \pi^+\pi^-\pi^-$ is used as an input to fix the parameter $\alpha_{\rm NR}$ defined in Eq. (2.7). Theoretical errors correspond to the uncertainties in (i) $\alpha_{\rm NR}$, (ii) $F_0^{B\pi}$, $\sigma_{\rm NR}$, and $m_s(\mu) = (90 \pm 20)$ MeV at $\mu = 2.1$ GeV, and (iii) $\gamma = (67.01^{+0.88}_{-1.99})^\circ$.

$B^- \to K^+K^-K^-$ Decay mode	*BABAR* [36]	Belle [37]	Theory
ϕK^-	$4.48 \pm 0.22^{+0.33}_{-0.24}$	$4.72 \pm 0.45 \pm 0.35^{+0.39}_{-0.22}$	$4.4^{+0.0+0.8+0.0}_{-0.0-0.7-0.0}$
$f_0(980)K^-$	$9.4 \pm 1.6 \pm 2.8$	< 2.9	$11.2^{+0.0+2.7+0.0}_{-0.0-2.1-0.0}$
$f_0(1500)K^-$	$0.74 \pm 0.18 \pm 0.52$		$0.63^{+0.0+0.11+0.0}_{-0.0-0.10-0.0}$
$f_0(1710)K^-$	$1.12 \pm 0.25 \pm 0.50$		$1.2^{+0+0.2+0}_{-0-0.2-0}$
$f_2'(1525)K^-$	$0.69 \pm 0.16 \pm 0.13$		
NR	$22.8 \pm 2.7 \pm 7.6$	$24.0 \pm 1.5 \pm 1.8^{+1.9}_{-5.7}$	$21.1^{+0.8+7.2+0.1}_{-1.1-5.7-0.1}$
Total	$33.4 \pm 0.5 \pm 0.9$	$30.6 \pm 1.2 \pm 2.3$	$28.8^{+0.5+7.9+0.1}_{-0.6-6.4-0.1}$
$B^- \to K^-\pi^+\pi^-$ Decay mode	*BABAR* [9]	Belle [10]	Theory
$\bar{K}^{*0}\pi^-$	$7.2 \pm 0.4 \pm 0.7^{+0.3}_{-0.5}$	$6.45 \pm 0.43 \pm 0.48^{+0.25}_{-0.35}$	$8.4^{+0.0+2.1+0.0}_{-0.0-1.9-0.0}$
$\bar{K}_0^{*0}(1430)\pi^-$	$19.8 \pm 0.7 \pm 1.7^{+5.6}_{-0.9} \pm 3.2$[a]	$32.0 \pm 1.0 \pm 2.4^{+1.1}_{-1.9}$	$11.5^{+0.0+3.3+0.0}_{-0.0-2.8-0.0}$
$\rho^0 K^-$	$3.56 \pm 0.45 \pm 0.43^{+0.38}_{-0.15}$	$3.89 \pm 0.47 \pm 0.29^{+0.32}_{-0.29}$	$2.9^{+0.0+0.7+0.0}_{-0.0-0.2-0.0}$
$f_0(980)K^-$	$10.3 \pm 0.5 \pm 1.3^{+1.5}_{-0.4}$	$8.78 \pm 0.82 \pm 0.65^{+0.55}_{-1.64}$	$6.7^{+0.0+1.6+0.0}_{-0.0-1.3-0.0}$
NR	$9.3 \pm 1.0 \pm 1.2^{+6.7}_{-0.4} \pm 1.2$	$16.9 \pm 1.3 \pm 1.3^{+1.1}_{-0.9}$	$15.7^{+0.0+8.1+0.0}_{-0.0-5.2-0.0}$
Total	$54.4 \pm 1.1 \pm 4.6$	$48.8 \pm 1.1 \pm 3.6$	$42.2^{+0.2+16.1+0.1}_{-0.1-10.7-0.1}$
$B^- \to K^+K^-\pi^-$ Decay mode	*BABAR* [46]	Belle [47]	Theory
$K^{*0}K^-$			$0.21^{+0.00+0.04+0.00}_{-0.00-0.04-0.00}$
$K_0^{*0}(1430)K^-$			$1.0^{+0.0+0.2+0.0}_{-0.0-0.2-0.0}$
$f_0(980)\pi^-$			$0.25^{+0.00+0.01+0.00}_{-0.00-0.01-0.00}$
NR			$2.9^{+0.7+0.6+0.0}_{-0.8-0.4-0.0}$
Total	5.0 ± 0.7	< 13	$5.2^{+0.8+1.0+0.0}_{-0.9-0.7-0.0}$
$B^- \to \pi^-\pi^+\pi^-$ Decay mode	*BABAR* [43]		Theory
$\rho^0\pi^-$	$8.1 \pm 0.7 \pm 1.2^{+0.4}_{-1.1}$		$7.3^{+0.0+0.4+0.0}_{-0.0-0.4-0.0}$
$\rho^0(1450)\pi^-$	$1.4 \pm 0.4 \pm 0.4^{+0.3}_{-0.7}$		
$f_0(1370)\pi^-$	$2.9 \pm 0.5 \pm 0.5^{+0.7}_{-0.5}$		$1.7^{+0.0+0.0+0.0}_{-0.0-0.0-0.0}$
$f_0(980)\pi^-$	< 1.5		$0.2^{+0.0+0.0+0.0}_{-0.0-0.0-0.0}$
NR	$5.3 \pm 0.7 \pm 0.6^{+1.1}_{-0.5}$		input
Total	$15.2 \pm 0.6 \pm 1.2^{+0.4}_{-0.3}$		$17.0^{+2.0+0.9+0.2}_{-2.3-0.7-0.2}$

[a]Recently, *BABAR* has measured the three-body decay $B^- \to K_S^0\pi^-\pi^0$ and obtained $\mathcal{B}(B^- \to \bar{K}_0^{*0}(1430)\pi^- \to K^-\pi^+\pi^-) = (31.0 \pm 3.0 \pm 3.8^{+1.7}_{-1.6}) \times 10^{-6}$ [3].

parametrization of the nonresonant amplitudes adopted in the *BABAR* and Belle analyses [37,45]

$$A_{\rm NR} = c_{12}e^{i\phi_{12}}e^{-\alpha s_{12}} + c_{13}e^{i\phi_{13}}e^{-\alpha s_{13}} + c_{23}e^{i\phi_{23}}e^{-\alpha s_{23}}. \tag{2.8}$$

We shall use the tree-dominated $B^- \to \pi^+\pi^-\pi^-$ decay data to fix the unknown parameter $\alpha_{\rm NR}$ as its nonresonant component is predominated by the transition process. Hence, the measurement of nonresonant contributions to $B^- \to \pi^+\pi^-\pi^-$ provides an ideal place to constrain the parameter $\alpha_{\rm NR}$, which turns out to be [5]

$$\alpha_{\rm NR} = 0.081^{+0.015}_{-0.009}\ {\rm GeV}^{-2}. \tag{2.9}$$

The phase ϕ_{12} of the nonresonant amplitude will be set to zero for simplicity.

Note that $A^{\rm HMChPT}_{\rm transition}$ receives nonresonant contributions from the whole Dalitz plot, including the central regions and regions near and along the edge. Since $p_B\cdot(p_1+p_2) = \frac{1}{2}(m_B^2 - m_3^2 + s_{12})$, it is obvious that the nonresonant signal $A_{\rm transition}$ arises mainly from the small invariant mass region of s_{12}.

For penguin-dominated decays $B \to KKK$ and $B \to K\pi\pi$, the nonresonant background induced from the $b \to u$ transition process yields $\mathcal{B}(B^- \to K^+K^-K^-)^{\rm NR} \sim 1.1\times 10^{-6}$ and $\mathcal{B}(B^- \to K^+\pi^+\pi^-)^{\rm NR} \sim 0.8\times 10^{-6}$, which are too small compared to experiment (see Table III). This is ascribed to the large CKM suppression $|V_{ub}V_{us}^*| \ll |V_{cb}V_{cs}^*| \approx |V_{tb}V_{ts}^*|$ associated with the $b \to u$ tree transition relative to the $b \to s$ penguin process. This implies that the two-body matrix element of scalar densities, e.g., $\langle K\bar{K}|\bar{s}s|0\rangle$ induced from the penguin diagram should have a large nonresonant component. The explicit expression of the nonresonant component of $\langle K\bar{K}|\bar{s}s|0\rangle$ will be shown in Eq. (2.17) below.

For the nonresonant contributions to the two-body matrix elements $\langle P_1P_2|\bar{q}\gamma_\mu q'|0\rangle$ and $\langle P_1P_2|\bar{q}q'|0\rangle$, we shall use the measured kaon electromagnetic form factors to extract $\langle K\bar{K}|\bar{q}\gamma_\mu q'|0\rangle^{\rm NR}$ and $\langle K\bar{K}|\bar{s}s|0\rangle^{\rm NR}$ first and then apply SU(3) symmetry to relate them to other two-body matrix elements [12].

B. Resonant contributions

In the experimental analysis of three-body decays, the resonant amplitude associated with the intermediate resonance R takes the form [48]

$$A_R = F_P \times F_R \times T_R \times W_R, \tag{2.10}$$

where T_R is usually described by a relativistic Breit-Wigner parametrization, W_R accounts for the angular distribution of the decay, F_P and F_R are the transition form factors of the parent particle and resonance, respectively (see, e.g., [48] for details).

In general, vector meson and scalar resonances contribute to the two-body matrix elements $\langle P_1P_2|V_\mu|0\rangle$ and $\langle P_1P_2|S|0\rangle$, respectively. The intermediate vector meson contributions to three-body decays are identified through the vector current, while the scalar meson resonances are mainly associated with the scalar density. Both scalar and vector resonances can contribute to the three-body matrix element $\langle P_1P_2|J_\mu|B\rangle$. Effects of intermediate resonances are described as a coherent sum of Breit-Wigner expressions. More precisely,[2]

$$\begin{aligned}
\langle P_1(p_1)P_2(p_2)|(\bar{q}b)_{V-A}|B\rangle^R &= \sum_i \langle P_1P_2|V_i\rangle \frac{1}{s_{12} - m_{V_i}^2 + im_{V_i}\Gamma_{V_i}} \langle V_i|(\bar{q}b)_{V-A}|B\rangle \\
&\quad + \sum_i \langle P_1P_2|S_i\rangle \frac{-1}{s_{12} - m_{S_i}^2 + im_{S_i}\Gamma_{S_i}} \langle S_i|(\bar{q}b)_{V-A}|B\rangle, \\
\langle P_1P_2|\bar{q}_1\gamma_\mu q_2|0\rangle^R &= \sum_i \langle P_1P_2|V_i\rangle \frac{1}{s_{12} - m_{V_i}^2 + im_{V_i}\Gamma_{V_i}} \langle V_i|\bar{q}_1\gamma_\mu q_2|0\rangle, \\
&\quad + \sum_i \langle P_1P_2|S_i\rangle \frac{-1}{s_{12} - m_{S_i}^2 + im_{S_i}\Gamma_{S_i}} \langle S_i|\bar{q}_1\gamma_\mu q_2|0\rangle, \\
\langle P_1P_2|\bar{q}_1 q_2|0\rangle^R &= \sum_i \langle P_1P_2|S_i\rangle \frac{-1}{s_{12} - m_{S_i}^2 + im_{S_i}\Gamma_{S_i}} \langle S_i|\bar{q}_1 q_2|0\rangle,
\end{aligned} \tag{2.11}$$

[2]Strictly speaking, for the $f_0(980)$ and $a_0(980)$, we should use the Flatté parametrization [49] to account for the threshold effect, though in practice we find that numerically it makes no significant difference from the use of the Breit-Wigner propagator.

where $V_i = \phi, \rho, \omega, \ldots$ and $S_i = f_0(980)$, $f_0(1370)$, $f_0(1500), \ldots$ for $P_1P_2 = \pi^+\pi^-$, and $V_i = K^*(892)$, $K^*(1410)$, $K^*(1680), \ldots$ and $S_i = K_0^*(1430), \ldots$ for $P_1P_2 = K^\pm\pi^\mp$. In general, the decay widths Γ_{V_i} and Γ_{S_i} are energy dependent. For $f_0(500)$ and $K_0^*(800)$, they are too broad to use the Breit-Wigner formulism.

Notice that the two-body matrix element $\langle P_1P_2|V_\mu|0\rangle$ can also receive contributions from scalar resonances when $q_1 \neq q_2$. For example, both K^* and $K_0^*(1430)$ contribute to the matrix element $\langle K^-\pi^+|\bar{s}\gamma_\mu d|0\rangle$ given by

$$\begin{aligned}\langle K^-(p_1)\pi^+(p_2)|\bar{s}\gamma_\mu d|0\rangle^R &= \sum_i \frac{g^{K_i^*\to K^-\pi^+}}{s_{12} - m_{K_i^*}^2 + i m_{K_i^*}\Gamma_{K_i^*}} \sum_{\rm pol} \varepsilon^* \cdot (p_1 - p_2)\langle K_i^*|\bar{s}\gamma_\mu d|0\rangle \\ &\quad - \sum_i \frac{g^{K_{0i}^*\to K^-\pi^+}}{s_{12} - m_{K_{0i}^*}^2 + i m_{K_{0i}^*}\Gamma_{K_{0i}^*}} \langle K_{0i}^*|\bar{s}\gamma_\mu d|0\rangle, \end{aligned} \tag{2.12}$$

with $K_i^* = K^*(892)$, $K^*(1410)$, $K^*(1680), \ldots$, and $K_{0i}^* = K_0^*(800)$, $K_0^*(1430), \ldots$.

C. Nonresonant contribution from matrix element of scalar density

Consider the nonresonant amplitude in the penguin-dominated $B^- \to K^+K^-K^-$ decay. In addition to the $b \to u$ tree transition which yields a rather small nonresonant fraction, we need to consider the nonresonant amplitudes indcued from the $b \to s$ penguin transition

$$\begin{aligned} A_1 &= \langle K^-(p_1)|(\bar{s}b)_{V-A}|B^-\rangle\langle K^+(p_2)K^-(p_3)|(\bar{q}q)_{V-A}|0\rangle, \\ A_2 &= \langle K^-(p_1)|\bar{s}b|B^-\rangle\langle K^+(p_2)K^-(p_3)|\bar{s}s|0\rangle, \end{aligned} \tag{2.13}$$

for $q = u, d, s$. The two-kaon matrix element created from the vacuum can be expressed in terms of timelike kaon current form factors as

$$\begin{aligned} \langle K^+(p_{K^+})K^-(p_{K^-})|\bar{q}\gamma_\mu q|0\rangle &= (p_{K^+} - p_{K^-})_\mu F_q^{K^+K^-}, \\ \langle K^0(p_{K^0})\bar{K}^0(p_{\bar{K}^0})|\bar{q}\gamma_\mu q|0\rangle &= (p_{K^0} - p_{\bar{K}^0})_\mu F_q^{K^0\bar{K}^0}. \end{aligned} \tag{2.14}$$

The weak vector form factors $F_q^{K^+K^-}$ and $F_q^{K^0\bar{K}^0}$ can be related to the kaon electromagnetic form factors $F_{\rm em}^{K^+K^-}$ and $F_{\rm em}^{K^0\bar{K}^0}$ for the charged and neutral kaons, respectively. As shown in [12], the nonresonant components of $F_q^{K^+K^-}$ read

$$\begin{aligned} F_{u,NR}^{K^+K^-} &= \frac{1}{3}(3F_{\rm NR} - F'_{\rm NR}), \qquad F_{d,NR}^{K^+K^-} = 0, \\ F_{s,NR}^{K^+K^-} &= -\frac{1}{3}(3F_{\rm NR} + 2F'_{\rm NR}), \end{aligned} \tag{2.15}$$

where the nonresonant terms $F_{\rm NR}$ and $F'_{\rm NR}$ can be parametrized as

$$F_{\rm NR}^{(\prime)}(s_{23}) = \left(\frac{x_1^{(\prime)}}{s_{23}} + \frac{x_2^{(\prime)}}{s_{23}^2}\right)\left[\ln\left(\frac{s_{23}}{\tilde{\Lambda}^2}\right)\right]^{-1}, \tag{2.16}$$

with $\tilde{\Lambda} \approx 0.3$ GeV. The unknown parameters x_i and x_i' are fitted from the kaon electromagnetic data, see [50] for details.

The nonresonant component of the matrix element of scalar density is given by [12][3]

$$\langle K^+(p_2)K^-(p_3)|\bar{s}s|0\rangle^{\rm NR} = \frac{v}{3}(3F_{\rm NR} + 2F'_{\rm NR}) + \sigma_{\rm NR}e^{-\alpha s_{23}}, \tag{2.17}$$

with

$$v = \frac{m_{K^+}^2}{m_u + m_s} = \frac{m_K^2 - m_\pi^2}{m_s - m_d}. \tag{2.18}$$

From the measured $\bar{B}^0 \to K_SK_SK_S$ rate and the K^+K^- mass spectrum measured in $\bar{B}^0 \to K^+K^-K_S$, the nonresonant $\sigma_{\rm NR}$ term can be constrained to be [12]

$$\sigma_{\rm NR} = e^{i\pi/4}(3.39^{+0.18}_{-0.21})\ {\rm GeV}. \tag{2.19}$$

For the parameter α appearing in Eq. (2.17), we will use the experimental measurement $\alpha = (0.14 \pm 0.02)\ {\rm GeV}^{-2}$ [52]. Numerically, the nonresonant signal is governed by the $\sigma_{\rm NR}$ component of the matrix element of scalar density. Owing to the exponential suppression factor $e^{-\alpha s_{ij}}$ in Eq. (2.17), the nonresonant contribution manifests in the low invariant mass regions.

D. Branching fractions

For numerical calculations, we follow [5] for the input parameters except the CKM matrix elements, which we will use the updated Wolfenstein parameters $A = 0.8227$, $\lambda = 0.22543$, $\bar{\rho} = 0.1504$, and $\bar{\eta} = 0.3540$ [53]. The corresponding CKM angles are $\sin 2\beta = 0.710 \pm 0.011$ and $\gamma = (67.01^{+0.88}_{-1.99})^\circ$ [53]. In Table III, we present updated branching fractions of resonant and nonresonant components in $B^- \to K^+K^-K^-$, $K^-\pi^+\pi^-$, $K^+K^-\pi^-$, and $\pi^-\pi^+\pi^-$ decays.

1. $B^- \to K^+K^-K^-$

As shown before in [5], the calculated $B^- \to K^-\phi \to K^-K^+K^-$ rate in the factorization approach is smaller than experiment. In the QCD factorization approach, this rate deficit problem calls for the $1/m_b$ power corrections from penguin annihilation. In this approach, it amounts

[3]Matrix elements of scalar densities (or scalar form factors) have also been studied in [51] within the framework of unitarized chiral perturbation theory and dispersion relations. However, the main focus there is on resonant contributions.

to replacing the penguin contribution characterized by $a_4^p \to a_4^p + \beta_3^p$, where $p = u$, c, and β_3 is the annihilation contribution induced mainly from $(S-P)(S+P)$ operators [54]. For our purpose, we will use

$$\beta_3^u[K\phi] = \beta_3^c[K\phi] = -0.0085 + 0.0088i. \tag{2.20}$$

This power correction $\beta_3^p[K\phi]$ is calculated in [55] for the quasi-two-body decay $B^- \to K^-\phi$. In principle, it should be computed in the three-body decay $B^- \to K^+K^-K^-$ with $m(K^+K^-)_{\rm low}$ peaked at the ϕ mass in QCDF. We will assume that $\beta_3^p[K\phi]$ calculated in either way is similar.

From Table III, it is clear that the predicted rates for the nonresonant component and for the total branching fraction of $B^- \to K^+K^-K^-$ are consistent with both *BABAR* and Belle analyses within errors.

2. $B^- \to K^-\pi^+\pi^-$

We first discuss resonant decays. From Table VI of [5], it is obvious that except for $f_0(980)K$, the predicted rates for penguin-dominated channels $K^*\pi$, $K_0^*(1430)\pi$, and ρK in $B^- \to K^-\pi^+\pi^-$ within the factorization approach are substantially smaller than the data by a factor of $2 \sim 5$. To overcome this problem, we shall use the penguin-annihilation induced power corrections calculated in our previous work [55]. The results are

$$\begin{aligned}\beta_3^p[\bar{K}^{*0}\pi^-] &= -0.032 + 0.022i,\\ \beta_3^p[\rho^0 K^-] &= 0.004 - 0.047i,\end{aligned} \tag{2.21}$$

for $p = u$, c. It is evident the discrepancy between theory and experiment for $\bar{K}^{*0}\pi^-$ and ρ^0K^- is greatly improved (see Table III).

As for the quasi-2-body mode $B^- \to \bar{K}_0^{*0}(1430)\pi^-$, *BABAR* Collaboration has recently measured the three-body decay $B^- \to K_S^0\pi^-\pi^0$ and obtained $\mathcal{B}(B^- \to \bar{K}_0^{*0}(1430)\pi^- \to K^-\pi^+\pi^-) = (31.0 \pm 3.0 \pm 3.8^{+1.6}_{-1.6}) \times 10^{-6}$ [3]. This is in good agreement with the Belle's result $(32.0 \pm 1.0 \pm 2.4^{+1.1}_{-1.9}) \times 10^{-6}$ [10]. Hence, the predicted rate by naive factorization is too small by a factor of 3. Indeed, this is still an unresolved puzzle even in both QCDF and pQCD approaches [56,57]. Using $\mathcal{B}(K_0^*(1430) \to K\pi) = 0.93$, we find $\mathcal{B}(B^- \to \bar{K}_0^{*0}(1430)\pi^-)_{\rm expt} \sim 51 \times 10^{-6}$, while QCDF predicts $(12.9^{+4.6}_{-3.7}) \times 10^{-6}$ [56]. This explains why our prediction of the total branching fraction of $B^- \to K^-\pi^+\pi^-$ is smaller than both *BABAR* and Belle analyses.

The nonresonant component of $B \to KKK$ is governed by the $K\bar{K}$ matrix element of scalar density $\langle K\bar{K}|\bar{s}s|0\rangle$. By the same token, the nonresonant contribution to the penguin-dominated $B \to K\pi\pi$ decays should be also dominated by the $K\pi$ matrix element of scalar density, namely $\langle K\pi|\bar{s}q|0\rangle$. When the unknown two-body matrix elements such as $\langle K^-\pi^+|\bar{s}d|0\rangle$ and $\langle \bar{K}^0\pi^-|\bar{s}u|0\rangle$, $\langle K^-\pi^0|\bar{s}u|0\rangle$ and $\langle \bar{K}^0\pi^0|\bar{s}d|0\rangle$ are related to $\langle K^+K^-|\bar{s}s|0\rangle$ via SU(3) symmetry, e.g.

$$\langle K^-(p_1)\pi^+(p_2)|\bar{s}d|0\rangle^{\rm NR} = \langle K^+(p_1)K^-(p_2)|\bar{s}s|0\rangle^{\rm NR}, \tag{2.22}$$

we find too large nonresonant and total branching fractions, namely, $\mathcal{B}(B^- \to K^-\pi^+\pi^-)_{\rm NR} \sim 29.7 \times 10^{-6}$ and $\mathcal{B}(B^- \to K^-\pi^+\pi^-)_{\rm tot} \sim 68.5 \times 10^{-6}$. Furthermore, Eq. (2.22) will lead to negative asymmetries $\mathcal{A}_{CP}^{\rm incl}(B^- \to K^-\pi^+\pi^-) \sim -0.8\%$ and $\mathcal{A}_{CP}^{\rm resc}(B^- \to K^-\pi^+\pi^-) \sim -6.4\%$, which are wrong in sign when confronted with the data. To accommodate the rates, it is tempting to assume that $\langle K^-\pi^+|\bar{s}d|0\rangle$ becomes slightly smaller because of SU(3) breaking. However, the predicted *CP* asymmetry is still not correct in sign. As argued in [5], we assumed that some sort of power corrections such as FSIs amount to giving a large strong phase δ to the nonresonant component of $\langle K^-\pi^+|\bar{s}d|0\rangle$

$$\begin{aligned}&\langle K^-(p_1)\pi^+(p_2)|\bar{s}d|0\rangle^{\rm NR}\\ &\quad = \frac{v}{3}(3F_{\rm NR} + 2F'_{\rm NR}) + \sigma_{\rm NR}e^{-\alpha s_{12}}e^{i\delta}.\end{aligned} \tag{2.23}$$

We found that $\delta \approx \pm\pi$ will enable us to accommodate both branching fractions and *CP* asymmetry simultaneously. In practice, we use

$$\begin{aligned}&\langle K^-(p_1)\pi^+(p_2)|\bar{s}d|0\rangle^{\rm NR}\\ &\quad \approx \frac{v}{3}(3F_{\rm NR} + 2F'_{\rm NR}) + \sigma_{\rm NR}e^{-\alpha s_{12}}e^{i\pi}\left(1 + 4\frac{m_K^2 - m_\pi^2}{s_{12}}\right).\end{aligned} \tag{2.24}$$

Our calculated nonresonant rate in $B^- \to K^-\pi^+\pi^-$ is consistent with the Belle measurement, but larger than that of *BABAR* analysis. It is of the same order of magnitude as that in $B^- \to K^+K^-K^-$ decays. Indeed, this is what we will expect. The reason why the nonresonant fraction is as large as 90% in *KKK* decays, but becomes only $17\% \sim 40\%$ in $K\pi\pi$ channels (see Table II) can be explained as follows. Since the *KKK* channel receives resonant contributions only from ϕ and f_0 mesons, while K^*, K_0^*, ρ, f_0 resonances contribute to $K\pi\pi$ modes, this explains why the nonresonant fraction is of order 90% in the former and becomes of order 40% or smaller in the latter.

Finally, we wish to stress again that the predicted total rate of $B^- \to K^-\pi^+\pi^-$ is smaller than the measurements of both *BABAR* and Belle analysis. This is ascribed to the fact that the calculated $K_0^*(1430)\pi^-$ in naive factorization is too small by a factor of 3.

3. $B^- \to K^+K^-\pi^-$

Applying U-spin symmetry to Eq. (2.24) leads to

$$\langle K^+(p_1)\pi^-(p_2)|\bar{d}s|0\rangle^{\rm NR} \approx \frac{v}{3}(3F_{\rm NR}+2F'_{\rm NR})+\sigma_{\rm NR}e^{-\alpha s_{12}}e^{i\pi}\left(1-4\frac{m_K^2-m_\pi^2}{s_{12}}\right), \tag{2.25}$$

which will be used to describe $B\to K\bar{K}\pi$ decays. Contrary to naive expectation, $s\bar{s}$ resonant contributions to the tree-dominated $B^-\to K^+K^-\pi^-$ decay are strongly suppressed. The only relevant factorizable amplitude which involves the $s\bar{s}$ current is given by [see Eq. (5.1) of [5]]

$$\langle\pi^-|(\bar{d}b)_{V-A}|B^-\rangle\langle K^+K^-|(\bar{s}s)_{V-A}|0\rangle \times\left[a_3+a_5-\frac{1}{2}(a_7+a_9)\right]. \tag{2.26}$$

The smallness of the penguin coefficients $a_{3,5,7,9}$ indicates negligible $s\bar{s}$ resonant contributions. Indeed, no clear $\phi(1020)$ signature is observed in the mass region $m^2_{K^+K^-}$ around 1 GeV^2 [7]. The branching fraction of the two-body decay $B^-\to\phi\pi^-$ is expected to be very small, of order 4.3×10^{-8}. It is induced mainly from $B^-\to\omega\pi^-$ followed by a small $\omega-\phi$ mixing [55].

The predicted nonresonant fraction is very sizable about 55% in $B^-\to K^+K^-\pi^-$ even it is a tree-dominated mode. This should be checked experimentally.

4. $B^-\to\pi^+\pi^-\pi^-$

The current-induced nonresonant contributions to the tree-dominated $B^-\to\pi^+\pi^-\pi^-$ decay are suppressed by the smallness of the penguin Wilson coefficients a_6 and a_8. Therefore, the nonresonant component of this decay is predominated by the transition process, and its measurement provides an ideal place to constrain the parameter $\alpha_{\rm NR}$.

5. Other $B\to K\pi\pi$ decays

Branching fractions of resonant and nonresonant (NR) contributions to other $B\to K\pi\pi$ decays such as $B^-\to\bar{K}^0\pi^-\pi^0$, $B^-\to K^-\pi^0\pi^0$, $\bar{B}^0\to\bar{K}^0\pi^+\pi^-$, and $\bar{B}^0\to K^-\pi^+\pi^0$ are shown in Table IV. Except the first channel, the other three have been studied before in [5]. In order to improve the discrepancy between theory and experiment for penguin-dominated VP modes in [5], we shall introduce penguin annihilation given in Eq. (2.21). In general, the predicted $K^*\pi$ and ρK rates are now consistent with experiment. However, the calculated $K_0^*(1430)\pi$ rates are still too small. This explains why the calculated total branching fractions are smaller than experiment, especially for $B^-\to\bar{K}^0\pi^-\pi^0$ due to the presence of two $K_0^*(1430)\pi$ modes.

In [5], we have made predictions for the resonant and nonresonant contributions to $\bar{B}^0\to\pi^+\pi^-\pi^0,\bar{K}^0\pi^0\pi^0$, $K_SK^\pm\pi^\mp$. The $\pi^+\pi^-\pi^0$ mode is predicted to have a rate larger than $\pi^+\pi^-\pi^-$ even though the former involves a π^0 and has no identical particles in the final state. This is because while the latter is dominated by the ρ^0 pole, the former receives $\rho^\pm$ and ρ^0 resonant contributions.

III. DIRECT CP ASYMMETRIES

Experimental measurements of inclusive and regional direct CP violation by LHCb for various charmless three-body B decays are collected in Table I. CP asymmetries of the pair $\pi^-\pi^+\pi^-$ and $K^-K^+K^-$ are of opposite signs, and likewise for the pair $K^-\pi^+\pi^-$ and $\pi^-K^+K^-$. This can be understood in terms of U-spin symmetry, which leads to the relation [16,19]

$$R_1\equiv\frac{\mathcal{A}_{CP}(B^-\to\pi^-\pi^+\pi^-)}{\mathcal{A}_{CP}(B^-\to K^-K^+K^-)}=-\frac{\Gamma(B^-\to K^-K^+K^-)}{\Gamma(B^-\to\pi^-\pi^+\pi^-)}, \tag{3.1}$$

and

$$R_2\equiv\frac{\mathcal{A}_{CP}(B^-\to\pi^-K^+K^-)}{\mathcal{A}_{CP}(B^-\to K^-\pi^+\pi^-)}=-\frac{\Gamma(B^-\to K^-\pi^+\pi^-)}{\Gamma(B^-\to\pi^-K^+K^-)}. \tag{3.2}$$

The predicted signs of the ratios R_1 and R_2 are confirmed by experiment. However, because of the momentum dependence of three-body decay amplitudes, U-spin or flavor SU(3) symmetry does not lead to any testable relations between $\mathcal{A}_{CP}(\pi^-K^+K^-)$ and $\mathcal{A}_{CP}(\pi^-\pi^+\pi^-)$ and between $\mathcal{A}_{CP}(K^-\pi^+\pi^-)$ and $\mathcal{A}_{CP}(K^+K^-K^-)$. That is, symmetry argument alone does not give hints at the relative sign of CP asymmetries in the pair of $\Delta S=0(1)$ decay.

The LHCb data in Table I indicate that decays involving a K^+K^- pair have a larger CP asymmetry ($\mathcal{A}_{CP}^{\rm incl}$ or $\mathcal{A}_{CP}^{\rm resc}$) than their partner channels. The asymmetries are positive for channels with a $\pi^+\pi^-$ pair and negative for those with a K^+K^- pair. In other words, when K^+K^- is replaced by $\pi^+\pi^-$, CP asymmetry is flipped in sign. This observation appears to imply that final-state rescattering may play an important role for direct CP violation. It has been conjectured that maybe the final rescattering between $\pi^+\pi^-$ and K^+K^- in conjunction with CPT invariance is responsible for the sign change [16,17,59]. However, the implication of the CPT theorem for CP asymmetries at the hadron level in exclusive or semi-inclusive reactions is more complicated and remains mostly unclear [60].

It is well-known that one needs nontrivial strong and weak phase differences to produce partial rate CP

TABLE IV. Branching fractions (in units of 10^{-6}) of resonant and nonresonant (NR) contributions to $B^- \to \bar{K}^0\pi^-\pi^0$, $B^- \to K^-\pi^0\pi^0$, $\bar{B}^0 \to \bar{K}^0\pi^+\pi^-$, and $\bar{B}^0 \to K^-\pi^+\pi^0$. Note that the *BABAR* result for $K_0^{*-}(1430)\pi^+$ in [39], all the *BABAR* results in [41] and Belle results in [42] are their absolute ones. We have converted them into the product branching fractions, namely, $\mathcal{B}(B \to Rh) \times \mathcal{B}(R \to hh)$.

$B^- \to \bar{K}^0\pi^-\pi^0$ Decay mode	*BABAR* [3]		Theory
$K^{*-}\pi^0$	$6.1 \pm 0.9 \pm 0.4^{+0.2}_{-0.3}$		$4.7^{+0.0+1.0+0.1}_{-0.0-0.9-0.1}$
$\bar{K}^{*0}\pi^-$	$4.9 \pm 0.9 \pm 0.4^{+0.2}_{-0.3}$		$4.1^{+0.0+1.0+0.0}_{-0.0-0.9-0.0}$
$K_0^{*-}(1430)\pi^0$	$10.7 \pm 1.5 \pm 0.9^{+0.0}_{-1.1}$		$5.6^{+0.0+1.6+0.0}_{-0.0-1.4-0.0}$
$\bar{K}_0^{*0}(1430)\pi^-$	$15.5 \pm 1.5 \pm 1.9^{+0.8}_{-0.8}$		$5.4^{+0.0+1.7+0.0}_{-0.0-1.4-0.0}$
$\rho^-\bar{K}^0$	$9.4 \pm 1.6 \pm 1.1^{+0.0}_{-2.6}$		$5.9^{+0.0+2.5+0.0}_{-0.0-0.9-0.0}$
NR			$9.5^{+0.3+6.3+0.0}_{-0.3-3.6-0.0}$
Total	$45.0 \pm 2.6 \pm 3.0^{+8.6}_{-0.0}$		$28.5^{+0.2+12.1+0.0}_{-0.3-7.4-0.0}$
$B^- \to K^-\pi^0\pi^0$ Decay mode	*BABAR* [58]		Theory
$K^{*-}\pi^0$	$2.7 \pm 0.5 \pm 0.4$		$2.5^{+0.0+0.6+0.0}_{-0.0-0.5-0.0}$
$K_0^{*-}(1430)\pi^0$			$2.4^{+0.0+0.8+0.0}_{-0.0-0.7-0.0}$
$f_0(980)K^-$	$2.8 \pm 0.6 \pm 0.5$		$3.3^{+0.0+0.8+0.0}_{-0.0-0.6-0.0}$
NR			$5.9^{+0.0+2.6+0.0}_{-0.0-1.9-0.0}$
Total	$16.2 \pm 1.2 \pm 1.5$		$13.3^{+0.1+4.6+0.0}_{-0.0-3.5-0.0}$
$\bar{B}^0 \to \bar{K}^0\pi^+\pi^-$ Decay mode	*BABAR* [39]	Belle [40]	Theory
$K^{*-}\pi^+$	$5.52^{+0.61}_{-0.54} \pm 0.35 \pm 0.41$	$5.6 \pm 0.7 \pm 0.5^{+0.4}_{-0.3}$	$6.8^{+0.0+1.7+0.1}_{-0.0-1.5-0.1}$
$K_0^{*-}(1430)\pi^+$	$18.5^{+1.4}_{-1.1} \pm 1.0 \pm 0.4 \pm 2.0$	$30.8 \pm 2.4 \pm 2.4^{+0.8}_{-3.0}$	$10.6^{+0.0+3.0+0.0}_{-0.0-2.6-0.0}$
$\rho^0\bar{K}^0$	$4.37^{+0.70}_{-0.61} \pm 0.29 \pm 0.12$	$6.1 \pm 1.0 \pm 0.5^{+1.0}_{-1.1}$	$3.9^{+0.0+1.9+0.0}_{-0.0-0.9-0.0}$
$f_0(980)\bar{K}^0$	$6.92 \pm 0.77 \pm 0.46 \pm 0.32$	$7.6 \pm 1.7 \pm 0.7^{+0.5}_{-0.7}$	$6.0^{+0.0+1.5+0.0}_{-0.0-1.2-0.0}$
$f_2(1270)\bar{K}^0$	$1.15^{+0.42}_{-0.35} \pm 0.11 \pm 0.35$		
NR	$11.1^{+2.5}_{-1.0} \pm 0.9$	$19.9 \pm 2.5 \pm 1.6^{+0.7}_{-1.2}$	$15.2^{+0.2+7.9+0.0}_{-0.2-5.2-0.0}$
Total	$50.2 \pm 1.5 \pm 1.8$	$47.5 \pm 2.4 \pm 3.7$	$40.0^{+0.1+16.9+0.1}_{-0.1-11.2-0.1}$
$\bar{B}^0 \to K^-\pi^+\pi^0$ Decay mode	*BABAR* [41]	Belle [42]	Theory
$K^{*-}\pi^+$	$2.7 \pm 0.4 \pm 0.3$	$4.9^{+1.5+0.5+0.8}_{-1.5-0.3-0.3}$	$3.5^{+0.0+0.9+0.1}_{-0.0-0.8-0.1}$
$\bar{K}^{*0}\pi^0$	$2.2 \pm 0.3 \pm 0.3$	< 2.3	$3.0^{+0.0+0.9+0.0}_{-0.0-0.8-0.0}$
$K_0^{*-}(1430)\pi^+$	$8.6 \pm 0.8 \pm 1.0$		$5.1^{+0.0+1.5+0.0}_{-0.0-1.3-0.0}$
$\bar{K}_0^{*0}(1430)\pi^0$	$4.3 \pm 0.3 \pm 0.7$		$4.2^{+0.0+1.4+0.0}_{-0.0-1.2-0.0}$
ρ^+K^-	$6.6 \pm 0.5 \pm 0.8$	$15.1^{+3.4+1.4+2.0}_{-3.3-1.5-2.1}$	$6.5^{+0.0+2.7+0.1}_{-0.0-1.1-0.1}$
NR	$7.6 \pm 0.5 \pm 1.0$	$5.7^{+2.7+0.5}_{-2.5-0.4} < 9.4$	$9.2^{+0.3+5.9+0.0}_{-0.4-3.4-0.0}$
Total	$38.5 \pm 1.0 \pm 3.9$	$36.6^{+4.2}_{-4.1} \pm 3.0$	$26.6^{+0.3+13.3+0.1}_{-0.4-7.8-0.1}$

asymmetries. In this work, the strong phases arise from the effective Wilson coefficients a_i^p listed in Eq. (2.3) of [5], the Breit-Wigner expression for resonances and the penguin matrix elements of scalar densities. It has been established that the strong phase in the penguin coefficients a_6^p and a_8^p comes from the Bander-Silverman-Soni mechanism [61]. There are two sources for the phase in the penguin matrix elements of scalar densities: $\sigma_{\rm NR}$ and δ for $K\pi$–vacuum matrix elements.

In the literature, most of the theory studies concentrate on the resonant effects on CP violation. For example, the authors of [16,18] considered the possibility of having a large local CP violation in $B^- \to \pi^+\pi^-\pi^-$ resulting from the interference of the resonances $f_0(500)$ and $\rho^0(770)$. A similar mechanism has been applied to the decay $B^- \to K^-\pi^+\pi^-$ [18].

In this work, we shall take into account both resonant and nonresonant amplitudes simultaneously and work out their contributions and interference to branching fractions and CP violation in details.

A. CP asymmetries due to resonant and nonresonant contributions

Following the framework of [5,12], we present in Table V the calculated results of inclusive and regional

TABLE V. Predicted inclusive and regional CP asymmetries (in %) for various charmless three-body B decays. Two local regions of interest for regional CP asymmetries are the low-mass regions specified in Eq. (1.1) for $\mathcal{A}_{CP}^{\rm incl}$ and the rescattering region of $m_{\pi\pi}$ and $m_{K\bar{K}}$ between 1.0 and 1.5 GeV for $\mathcal{A}_{CP}^{\rm resc}$. Resonant (RES) and nonresonant (NR) contributions to direct CP asymmetries are considered.

	$\pi^-\pi^+\pi^-$	$K^+K^-\pi^-$	$K^-\pi^+\pi^-$	$K^+K^-K^-$
$(\mathcal{A}_{CP}^{\rm incl})_{\rm NR}$	$25.0^{+4.4+2.1+0.0}_{-2.7-3.1-0.1}$	$-25.6^{+2.2+1.7+0.2}_{-3.0-1.1-0.1}$	$9.1^{+1.3+2.2+0.1}_{-1.8-2.0-0.1}$	$-7.8^{+1.4+1.3+0.1}_{-0.9-1.5-0.1}$
$(\mathcal{A}_{CP}^{\rm incl})_{\rm RES}$	$5.3^{+0.0+1.6+0.0}_{-0.0-1.3-0.0}$	$-16.3^{+0.0+0.9+0.1}_{-0.0-0.8-0.1}$	$6.9^{+0.0+2.1+0.1}_{-0.0-1.8-0.1}$	$1.2^{+0.0+0.0+0.0}_{-0.0-0.0-0.0}$
$(\mathcal{A}_{CP}^{\rm incl})_{\rm NR+RES}$	$8.3^{+0.5+1.6+0.0}_{-1.1-1.5-0.0}$	$-10.2^{+1.6+1.5+0.1}_{-2.5-1.4-0.1}$	$7.3^{+0.2+2.1+0.1}_{-0.2-2.0-0.1}$	$-6.0^{+1.8+0.8+0.1}_{-1.2-0.9-0.1}$
$(\mathcal{A}_{CP}^{\rm incl})_{\rm expt}$	5.8 ± 2.4	-12.3 ± 2.2	2.5 ± 0.9	-3.6 ± 0.8
$(\mathcal{A}_{CP}^{\rm low})_{\rm NR}$	$58.3^{+3.6+2.6+0.8}_{-3.7-4.0-0.8}$	$-25.0^{+2.8+2.7+0.3}_{-5.4-2.5-0.3}$	$48.9^{+7.0+7.6+0.3}_{-10.5-8.2-0.3}$	$-13.0^{+2.0+2.8+0.2}_{-1.2-3.2-0.2}$
$(\mathcal{A}_{CP}^{\rm low})_{\rm RES}$	$4.5^{+0.0+1.6+0.0}_{-0.0-1.2-0.0}$	$-4.9^{+0.0+0.5+0.0}_{-0.0-0.4-0.0}$	$57.1^{+0.0+7.9+0.9}_{-0.0-16.6-0.9}$	$1.6^{+0.0+0.1+0.0}_{-0.0-0.1-0.0}$
$(\mathcal{A}_{CP}^{\rm low})_{\rm NR+RES}$	$21.9^{+0.5+3.0+0.0}_{-0.4-3.3-0.1}$	$-17.5^{+0.6+1.7+0.1}_{-0.9-1.5-0.1}$	$49.4^{+0.7+9.4+0.8}_{-1.0-14.2-0.8}$	$-16.8^{+3.5+2.8+0.2}_{-2.3-3.2-0.2}$
$(\mathcal{A}_{CP}^{\rm low})_{\rm expt}$	58.4 ± 9.7	-64.8 ± 7.2	67.8 ± 8.5	-22.6 ± 2.2
$(\mathcal{A}_{CP}^{\rm resc})_{\rm NR}$	$36.7^{+6.2+3.2+0.1}_{-3.7-4.6-0.2}$	$-27.7^{+3.1+3.0+0.4}_{-5.9-2.7-0.4}$	$31.8^{+4.6+4.6+0.3}_{-6.7-4.5-0.3}$	$-10.8^{+1.8+2.2+0.2}_{-1.2-2.5-0.2}$
$(\mathcal{A}_{CP}^{\rm resc})_{\rm RES}$	$7.0^{+0.0+1.8+0.0}_{-0.0-1.5-0.0}$	$-5.6^{+0.0+0.5+0.0}_{-0.0-0.4-0.0}$	$1.1^{+0.0+0.6+0.0}_{-0.0-0.5-0.0}$	$0.96^{+0.00+0.02+0.01}_{-0.00-0.02-0.01}$
$(\mathcal{A}_{CP}^{\rm resc})_{\rm NR+RES}$	$13.4^{+0.5+2.0+0.0}_{-1.1-2.1-0.0}$	$-20.4^{+1.2+2.0+0.2}_{-1.8-1.8-0.2}$	$4.1^{+0.2+0.9+0.0}_{-0.3-0.9-0.0}$	$-3.8^{+1.5+0.5+0.1}_{-1.0-0.5-0.1}$
$(\mathcal{A}_{CP}^{\rm resc})_{\rm expt}$	17.2 ± 2.7	-32.8 ± 4.1	12.1 ± 2.2	-21.1 ± 1.4

CP asymmetries in our model. We consider both resonant and nonresonant mechanisms and their interference. For nonresonant contributions, direct CP violation arises solely from the interference of tree and penguin nonresonant amplitudes. For example, in the absence of resonances, CP asymmetry in $B^- \to K^-\pi^+\pi^-$ stems mainly from the interference of the nonresonant tree amplitude $\langle\pi^+\pi^-|(\bar{u}b)_{V-A}|B^-\rangle^{\rm NR}\langle K^-|(\bar{s}u)_{V-A}|0\rangle$ and the nonresonant penguin amplitude $\langle\pi^-|\bar{d}b|B^-\rangle\langle K^-\pi^+|\bar{s}d|0\rangle^{\rm NR}$.

It is clear from Table V that nonresonant CP violation is usually much larger than the resonant one and that the interference effect is generally quite significant. If nonresonant contributions are turned off in the $K^+K^-K^-$ mode, the predicted asymmetries will be wrong in sign when compared with experiment. This is not a surprise because $B^- \to K^+K^-K^-$ is predominated by the nonresonant background. The magnitude and the sign of its CP asymmetry should be governed by the nonresonant term.

Large local CP asymmetries $\mathcal{A}_{CP}^{\rm low}$ in three-body charged B decays have been observed by LHCb in the low mass regions specified in Eq. (1.1). If intermediate resonant states are not associated in these low-mass regions, it is natural to expect that the Dalitz plot is governed by nonresonant contributions. It is evident from Table V that except the mode $K^+K^-\pi^-$, CP violation in the low mass region is indeed dominated by the nonresonant background. In our model, we find large nonresonant contributions to CP asymmetries for $B^- \to \pi^+\pi^-\pi^-, \pi^+\pi^-K^-$, of order 0.58 and 0.49, respectively. Likewise, large $(\mathcal{A}_{CP}^{\rm low})_{\rm NR} = (51.9^{+1.08+0.27}_{-0.91-0.32})\%$ for the former mode was also obtained in the pQCD approach [22].

From Table V, it is evident that except the $K^+K^-K^-$ mode, the resonant contributions to integrated inclusive CP asymmetries are of the same sign and similar magnitudes as $\mathcal{A}_{CP}^{\rm incl}$. For $\pi^+\pi^-\pi^-$, resonant CP violation is dominated by the ρ^0, $\mathcal{A}_{CP}(\rho^0\pi^-) = 0.059^{+0.012}_{-0.010}$, which is close to the resonance-induced integrated asymmetry $(\mathcal{A}_{CP}^{\rm incl})_{\rm RES} = (5.3^{+1.6}_{-1.3})\%$. However, there is an issue about the theoretical predictions of $\mathcal{A}_{CP}(\rho^0\pi^-)$, which will be addressed in detail below. The resonant CP asymmetry in $B^- \to K^-\pi^+\pi^-$ is governed by the ρ^0 with $\mathcal{A}_{CP}(\rho^0K^-) = 0.65^{+0.10}_{-0.21}$, while the world average of measurements is 0.37 ± 0.11 [2]. For $K^+K^-\pi^-$, we have the dominant contributions from $\mathcal{A}_{CP}(K^{*0}K^-) = -28.4\%$ and $\mathcal{A}_{CP}(K_0^{*0}(1430)K^-) = -19.2\%$. For $K^+K^-K^-$, the main contributions to $(\mathcal{A}_{CP}^{\rm incl})_{\rm RES}$ arise from $\phi K^-, f_0(1500)K^-$, $f_0(1710)K^-$, all give positive contributions. The observed negative $\mathcal{A}_{CP}^{\rm incl}(K^+K^-K^-)$ is a strong indication of the importance of nonresonant effects. This is reinforced by the fact that the predicted $(\mathcal{A}_{CP}^{\rm low})_{\rm RES}$ and $(\mathcal{A}_{CP}^{\rm resc})_{\rm RES}$ by resonances alone are usually too small compared to the data, especially for the former.

B. Discussions

Although our model based on factorization describes the observed asymmetries reasonably well, in the following, we would like to address several related issues.

1. CP asymmetry induced by interference

CP asymmetry of the $B^- \to \pi^+\pi^-\pi^-$ decay in the low-mass region of $m(\pi^+\pi^-)_{\rm low}$ is observed to change sign at a value of $m(\pi^+\pi^-)_{\rm low}$ close to the $\rho(770)$ resonance. This change of sign occurs for both $\cos\theta > 0$ and $\cos\theta < 0$ (see Fig. 4 of [8]), where θ is the angle between the momenta of

the unpaired hadron and the resonance decay product with the same-sign charge. Likewise, the Dalitz CP asymmetry of $B^- \to K^-\pi^+\pi^-$ has two zeros in the $m(\pi^+\pi^-)$ distribution. In the $\cos\theta < 0$ region, there is a zero around the $\rho(770)$ mass and another one around the $f_0(980)$ meson mass (see Fig. 5 of [8]). However, in the region of $\cos\theta > 0$, a clear change of sign is only seen around the $f_0(980)$ mass.

In this work, we do see the sign change of CP asymmetry in the decay $B^- \to \pi^+\pi^-\pi^-$ for $\cos\theta < 0$ but not for $\cos\theta > 0$. The former arises from the interference of $\rho(770)$ with the nonresonant background. The sign change is ascribed to the real part of the Breit-Wigner propagator of the $\rho(770)$, which reads

$$\frac{s - m_\rho^2}{(s - m_\rho^2)^2 + m_\rho^2\Gamma_\rho^2(s)}. \tag{3.3}$$

It is not clear to us why we did not see the zero for $\cos\theta > 0$. As for $B^- \to K^-\pi^+\pi^-$, the interference between $\rho(770)$ and $f_0(980)$ has a real component proportional to

$$\frac{(s - m_\rho^2)(s - m_{f_0}^2)}{[(s - m_\rho^2)^2 + m_\rho^2\Gamma_\rho^2(s)][(s - m_{f_0}^2)^2 + m_{f_0}^2\Gamma_{f_0}^2(s)]}. \tag{3.4}$$

This gives two zeros: one at $s = m^2_{\rho(770)}$ and the other at $s = m^2_{f_0(980)}$. However, we only see a sign change around $f_0(980)$ but not $\rho(770)$ for $\cos\theta < 0$ and do not see any zero for $\cos\theta > 0$. It is possible that the zeros are contaminated or washed out by other contributions. We are going to investigate this issue.

2. Strong phase δ

We now discuss in more detail why we need to introduce an additional phase δ to the matrix element of scalar density $\langle K^-\pi^+|\bar{s}d|0\rangle$ given in Eq. (2.23). First, we notice that the calculated integrated CP asymmetries $(8.3^{+1.7}_{-1.9})\%$ for $\pi^+\pi^-\pi^-$ and $(-6.0^{+2.0}_{-1.5})\%$ for $K^+K^-K^-$ (see Table V) are consistent with LHC measurements in both sign and magnitude.[4] As discussed in passing and in [5], when the unknown two-body matrix elements of scalar densities $\langle K\pi|\bar{s}q|0\rangle$ and $\langle \pi K|\bar{s}q|0\rangle$ are related to $\langle K\bar{K}|\bar{s}s|0\rangle$ via SU(3) symmetry so that $\langle K^-\pi^+|\bar{s}d|0\rangle = \langle K^+\pi^-|\bar{d}s|0\rangle = \langle K^+K^-|\bar{s}s|0\rangle$, the calculated nonresonant and total rates of $B^- \to K^-\pi^+\pi^-$ will be too large compared to experiment [see the discussions after Eq. (2.22)]. Moreover, the predicted CP violation $\mathcal{A}_{CP}^{\rm incl}(K^-\pi^+\pi^-) = (-0.8^{+0.9}_{-0.6})\%$ and $\mathcal{A}_{CP}^{\rm incl}(K^+K^-\pi^-) = (4.9^{+1.1}_{-1.0})\%$ are wrong in sign when confronted with experiment. Since the partial rate asymmetry arises from the interference between tree and penguin amplitudes and since nonresonant penguin contributions to the penguin-dominated decay $K^-\pi^+\pi^-$ are governed by the matrix element $\langle K^-\pi^+|\bar{s}d|0\rangle$, it is thus conceivable that a strong phase δ in $\langle K^-\pi^+|\bar{s}d|0\rangle$ induced from some sort of power corrections might flip the sign of CP asymmetry.

It is clear from Table VI that the reason why the predicted inclusive and regional CP asymmetries [except $\mathcal{A}_{CP}^{\rm low}(K^-\pi^+\pi^-)$] all are erroneous in sign when δ is set to zero is ascribed to the nonresonant contributions, which are opposite in sign to the experimental measurements. By comparing Tables VI and V, we see that when δ is set to $\approx \pm\pi$ preferred by the data, CP asymmetries induced from nonresonant components will flip the sign as $e^{\pm i\pi} = -1$. Consequently, this in turn will lead to the correct sign for the predicted asymmetries. As stressed in [5], we have implicitly assumed that power corrections will not affect CP violation in $\pi^+\pi^-\pi^-$ and $K^+K^-K^-$.

Finally, we would like to remark that unlike the global weak phases, strong phases such as δ and the Breit-Wigner phase are local ones, namely, they are energy and channel dependent. For example, when we study CP-asymmetry Dalitz distributions in some large invariant mass regions (see Sec. III. 4 below), we find that δ needs to vanish in the large invariant mass region for $B^- \to K^+K^-\pi^-$ in order to accommodate the observation.

3. Final-state rescattering

As shown in Table VI, the calculated integrated and local CP asymmetries $\mathcal{A}_{CP}^{\rm incl}$, $\mathcal{A}_{CP}^{\rm low}$, and $\mathcal{A}_{CP}^{\rm resc}$ for $B^- \to K^+K^-\pi^-, K^-\pi^+\pi^-$ with $\delta = 0$ are wrong in sign when

TABLE VI. Same as Table V except that the strong phase δ defined in Eq. (2.23) for $K\pi$ matrix element of scalar density is set to zero. The decays $B^- \to \pi^+\pi^-\pi^-$ and $K^+K^-K^-$ are not affected by the phase δ.

	$K^+K^-\pi^-$	$K^-\pi^+\pi^-$
$(\mathcal{A}_{CP}^{\rm incl})_{\rm NR}$	$17.4^{+0.7+1.7+0.0}_{-1.0-2.9-0.1}$	$-3.5^{+0.8+1.1+0.1}_{-0.6-1.3-0.0}$
$(\mathcal{A}_{CP}^{\rm incl})_{\rm RES}$	$-16.3^{+0.0+0.9+0.1}_{-0.0-0.8-0.1}$	$6.9^{+0.0+2.1+0.1}_{-0.0-1.8-0.1}$
$(\mathcal{A}_{CP}^{\rm incl})_{\rm NR+RES}$	$4.9^{+0.7+0.9+0.1}_{-0.8-0.6-0.1}$	$-0.8^{+0.7+0.6+0.0}_{-0.5-0.3-0.0}$
$(\mathcal{A}_{CP}^{\rm incl})_{\rm expt}$	-12.3 ± 2.2	2.5 ± 0.9
$(\mathcal{A}_{CP}^{\rm low})_{\rm NR}$	$22.3^{+5.3+2.6+0.0}_{-2.8-2.9-0.1}$	$-19.0^{+1.5+5.0+0.4}_{-0.7-5.9-0.3}$
$(\mathcal{A}_{CP}^{\rm low})_{\rm RES}$	$-4.9^{+0.0+0.5+0.0}_{-0.0-0.4-0.0}$	$57.1^{+0.0+7.9+0.9}_{-0.0-16.6-0.9}$
$(\mathcal{A}_{CP}^{\rm low})_{\rm NR+RES}$	$4.6^{+0.7+0.6+0.0}_{-0.4-0.8-0.0}$	$40.7^{+3.2+5.0+0.3}_{-2.4-8.6-0.4}$
$(\mathcal{A}_{CP}^{\rm low})_{\rm expt}$	-64.8 ± 7.2	67.8 ± 8.5
$(\mathcal{A}_{CP}^{\rm resc})_{\rm NR}$	$25.2^{+5.9+2.8+0.0}_{-3.1-3.2-0.1}$	$-11.5^{+1.6+3.2+0.2}_{-0.9-3.8-0.2}$
$(\mathcal{A}_{CP}^{\rm resc})_{\rm RES}$	$-5.6^{+0.0+0.5+0.0}_{-0.0-0.4-0.0}$	$1.1^{+0.0+0.6+0.0}_{-0.0-0.5-0.0}$
$(\mathcal{A}_{CP}^{\rm resc})_{\rm NR+RES}$	$10.1^{+1.2+1.3+0.0}_{-0.7-1.5-0.1}$	$-6.4^{+1.0+0.3+0.1}_{-0.7-0.1-0.1}$
$(\mathcal{A}_{CP}^{\rm resc})_{\rm expt}$	-32.8 ± 4.1	12.1 ± 2.2

[4]Before the LHCb measurements of CP violation in three-body B decays, the predicted CP asymmetries in various charmless three-body B decays can be found in Table XVII of [12].

confronted with experiment. Since direct CP violation in charmless two-body B decays can be significantly affected by final-state rescattering [62], it is natural to hope that final-state rescattering effects in three-body B decays may resolve the discrepancy. For example, the sign of the CP asymmetry in the two-body decay $\bar{B}^0 \to K^-\pi^+$ can be flipped by the presence of long-distance rescattering of charming penguins [62].

Just as the example of $\bar{B}^0 \to K^-\pi^+$, whose CP violation is originally predicted to have the wrong sign in naive factorization and gets a correct sign after power corrections such as final-state interactions or penguin annihilation, are taken into account, it will be very interesting to see an explicit demonstration of the sign flip of $\mathcal{A}_{CP}(K^-\pi^+\pi^-)$ and $\mathcal{A}_{CP}(\pi^-K^+K^-)$ when the final-state rescattering of $\pi\pi \leftrightarrow K\bar{K}$ is turned on.

Here, we shall follow the work of [63] (also the same framework adapted in [26]) to describe the inelastic $\pi\pi \leftrightarrow K\bar{K}$ rescattering process and consider this final-state rescattering effect on inclusive and local CP violation.

The general expression of three-body B decay amplitude under final-state interactions is given by [64,65]

$$A_i^{\rm FSI} = \sum_{j=1}^{n} (S^{1/2})_{ij} A_j^{\rm fac}. \tag{3.5}$$

We now concentrate on $\pi^+\pi^-$ and K^+K^- final-state rescattering and neglect possible interactions with the third meson under the so-called "2 + 1" assumption and write

$$\begin{pmatrix} A(B^- \to \pi^+\pi^- P^-) \\ A(B^- \to K^+K^- P^-) \end{pmatrix}^{\rm FSI} = S^{1/2} \begin{pmatrix} A(B^- \to \pi^+\pi^- P^-) \\ A(B^- \to K^+K^- P^-) \end{pmatrix} \tag{3.6}$$

with $P = \pi, K$. The unitary S matrix reads

$$S = \begin{pmatrix} \eta e^{2i\delta_{\pi\pi}} & i\sqrt{1-\eta^2}\, e^{i(\delta_{\pi\pi}+\delta_{K\bar{K}})} \\ i\sqrt{1-\eta^2}\, e^{i(\delta_{\pi\pi}+\delta_{K\bar{K}})} & \eta e^{2i\delta_{K\bar{K}}} \end{pmatrix}, \tag{3.7}$$

where the inelasticity parameter $\eta(s)$ is given by [63]

$$\eta(s) = 1 - \left(\epsilon_1 \frac{k_2}{s^{1/2}} + \epsilon_2 \frac{k_2^2}{s}\right) \frac{M'^2 - s}{s}, \tag{3.8}$$

with

$$k_2 = \frac{\sqrt{s - 4m_K^2}}{2}. \tag{3.9}$$

The $\pi\pi$ phase shift has the expression

$$\delta_{\pi\pi}(s) = \frac{1}{2}\cos^{-1}\left(\frac{\cot^2[\delta_{\pi\pi}(s)] - 1}{\cot^2[\delta_{\pi\pi}(s)] + 1}\right), \tag{3.10}$$

with

$$\cot[\delta_{\pi\pi}(s)] = c_0 \frac{(s - M_s^2)(M_f^2 - s)}{M_f^2 s^{1/2}} \frac{|k_2|}{k_2^2}. \tag{3.11}$$

We shall assume that $\delta_{K\bar{K}} \approx \delta_{\pi\pi}$ in the rescattering region.

To calculate $S^{1/2}$, we note that the S matrix can be recast to the form

$$\begin{aligned} S &= U \begin{pmatrix} \eta e^{2i\delta_{\pi\pi}}\left(\eta - i\sqrt{1-\eta^2}\right) & 0 \\ 0 & \eta e^{2i\delta_{\pi\pi}}\left(\eta + i\sqrt{1-\eta^2}\right) \end{pmatrix} U^\dagger \\ &= U e^{2i\delta_{\pi\pi}} \begin{pmatrix} e^{-i\phi} & 0 \\ 0 & e^{i\phi} \end{pmatrix} U^\dagger, \end{aligned} \tag{3.12}$$

with

$$U = \frac{1}{\sqrt{2}} \begin{pmatrix} 1 & 1 \\ -1 & 1 \end{pmatrix} \tag{3.13}$$

and

$$\phi = \tan^{-1} \frac{\sqrt{1-\eta^2}}{\eta}. \tag{3.14}$$

Hence,

$$\begin{aligned} S^{1/2} &= U e^{i\delta_{\pi\pi}} \begin{pmatrix} e^{-i\phi/2} & 0 \\ 0 & e^{i\phi/2} \end{pmatrix} U^\dagger \\ &= e^{i\delta_{\pi\pi}} \begin{pmatrix} \cos\phi/2 & i\sin\phi/2 \\ i\sin\phi/2 & \cos\phi/2 \end{pmatrix}. \end{aligned} \tag{3.15}$$

Consequently,

$$\begin{aligned} A(B^- \to \pi^+\pi^- P^-)^{\rm FSI} &= e^{i\delta_{\pi\pi}}[\cos(\phi/2) A(B^- \to \pi^+\pi^- P^-) \\ &\quad + i\sin(\phi/2) A(B^- \to K^+K^- P^-)], \\ A(B^- \to K^+K^- P^-)^{\rm FSI} &= e^{i\delta_{\pi\pi}}[\cos(\phi/2) A(B^- \to K^+K^- P^-) \\ &\quad + i\sin(\phi/2) A(B^- \to \pi^+\pi^- P^-)], \end{aligned} \tag{3.16}$$

for $P = \pi, K$.

For the numerical results presented in Table VII, we have used the parameters given in Eqs. (2.15b') and (2.16) of [63], namely, $M' = 1.5$ GeV, $M_s = 0.92$ GeV, $M_f = 1.32$ GeV, $\epsilon_1 = 2.4$, $\epsilon_2 = -5.5$, and $c_0 = 1.3$. Unfortunately, our results are rather disappointing: in the presence of the specific final-state rescattering, CP asymmetries for both $\pi^+\pi^-\pi^-$ and $K^+K^-\pi^-$ are heading in the wrong direction. While $\mathcal{A}_{CP}$ is decreased for the former, it is increased for the latter, rendering the discrepancy

TABLE VII. Predicted inclusive and regional CP asymmetries (in %) for various charmless three-body B decays in the presence of $\pi^+\pi^- \leftrightarrow K^+K^-$ final-state rescattering. We have set δ to zero. Only the central values of the final-state interaction (FSI) effects are quoted here.

	$\pi^-\pi^+\pi^-$	$K^+K^-\pi^-$	$K^-\pi^+\pi^-$	$K^+K^-K^-$
$(\mathcal{A}_{CP}^{\rm incl})_{\rm NR+RES}$	$8.3^{+0.3+1.6+0.0}_{-1.1-1.5-0.0}$	$4.9^{+0.7+0.9+0.1}_{-0.8-0.6-0.1}$	$-0.8^{+0.7+0.6+0.0}_{-0.5-0.3-0.0}$	$-6.0^{+1.8+0.8+0.1}_{-1.2-0.9-0.1}$
$(\mathcal{A}_{CP}^{\rm incl})_{\rm NR+RES+FSI}$	-15.6	8.1	0.7	-6.1
$(\mathcal{A}_{CP}^{\rm incl})_{\rm expt}$	5.8 ± 2.4	-12.3 ± 2.2	2.5 ± 0.9	-3.6 ± 0.8
$(\mathcal{A}_{CP}^{\rm low})_{\rm NR+RES}$	$21.9^{+0.5+3.0+0.0}_{-0.4-3.3-0.1}$	$4.6^{+0.7+0.6+0.0}_{-0.4-0.8-0.0}$	$40.7^{+3.2+5.0+0.3}_{-2.4-8.6-0.4}$	$-16.8^{+3.5+2.8+0.2}_{-2.3-3.2-0.2}$
$(\mathcal{A}_{CP}^{\rm low})_{\rm NR+RES+FSI}$	-17.6	13.2	2.3	-16.7
$(\mathcal{A}_{CP}^{\rm low})_{\rm expt}$	58.4 ± 9.7	-64.8 ± 7.2	67.8 ± 8.5	-22.6 ± 2.2
$(\mathcal{A}_{CP}^{\rm resc})_{\rm NR+RES}$	$13.4^{+0.5+2.0+0.0}_{-1.1-2.1-0.0}$	$10.1^{+1.2+1.3+0.0}_{-0.7-1.5-0.1}$	$-6.4^{+1.0+0.3+0.1}_{-0.7-0.1-0.1}$	$-3.8^{+1.5+0.5+0.1}_{-1.0-0.5-0.1}$
$(\mathcal{A}_{CP}^{\rm resc})_{\rm NR+RES+FSI}$	10.4	20.0	-1.3	-4.0
$(\mathcal{A}_{CP}^{\rm resc})_{\rm expt}$	17.2 ± 2.7	-32.8 ± 4.1	12.1 ± 2.2	-21.1 ± 1.4

between theory and experiment even worse. We also see that $\mathcal{A}_{CP}(K^+K^-K^-)$ is almost not affected by the rescattering of $\pi\pi$ and $K\bar{K}$.

Thus far, we have confined ourselves to rescattering between $\pi^+\pi^-$ and K^+K^- in s-wave configuration. It is known from two-body B decays that this particular rescattering channel (through annihilation and total annihilation diagrams, see Fig. 1 of [64]) cannot be sizeable, or the rescattered $B^0 \to K^+K^-$ rate fed from the $B^0 \to \pi^+\pi^-$ mode will easily excess the measured rate, which is highly suppressed [1]. In fact, the effect of exchange rescattering is expected to be more prominent [64], and one needs to enlarge the rescattering channels. It is clear that $\pi\pi$ and KK are not confined to the s-wave configuration in the three-body decays. Therefore, rescatterings in other partial wave configurations should also be included. Rescatterings between the third meson and other mesons can be relevant. Moreover, other potentially important coupled channels should not be neglected. For example, the decay $B^- \to \pi^+\pi^-\pi^-$ can be produced through the weak decay $B \to D\bar{D}^*\pi$ followed by the rescattering of $D\bar{D}^*\pi \to \pi\pi\pi$ and likewise for other three-body decays of B mesons. The intermediate $D_{(s)}^{(*)}\bar{D}_{(s)}^{(*)}P$ states have large CKM matrix elements and hence can make significant contributions to CP violation when coupled to three light pseudoscalar states.

A comprehensive study of rescattering effects in three-body B decays is beyond the scope of the present work. At any rate, in this work, we shall use the phenomenological phase $\delta \approx \pm\pi$ to describe the decays and CP violation of $B^- \to K^+K^-\pi^-, K^-\pi^+\pi^-$.

4. CP violation in $B^- \to \rho^0\pi^-$

It has been claimed that the observed large localized CP violation in $B^- \to \pi^+\pi^-\pi^-$ may result from the interference of a light scalar meson $f_0(500)$ and the vector $\rho^0(770)$ resonance [16,18], even though the latter one is not covered in the low mass region $m^2_{\pi^+\pi^-\,\rm low} < 0.4\ {\rm GeV}^2$. Let us consider the intermediate state ρ^0 in the $B^- \to \pi^+\pi^-\pi^-$ decay. As shown in Table III, the calculated $\mathcal{B}(B^- \to \rho^0\pi^-) = (7.3 \pm 0.4) \times 10^{-6}$ is consistent with the world average $(8.3^{+1.2}_{-1.3}) \times 10^{-6}$ [2] within errors. Its CP asymmetry is found to be $\mathcal{A}_{CP}(\rho^0\pi^-) = 0.059^{+0.012}_{-0.010}$. At first sight, this seems to be in agreement in sign with the *BABAR* measurement $0.18 \pm 0.07^{+0.05}_{-0.15}$ from the Dalitz plot analysis of $B^- \to \pi^+\pi^-\pi^-$ [43]. However, theoretical predictions based on QCDF, pQCD, and SCET all lead to a negative CP asymmetry of order -0.20 for $B^- \to \rho^0\pi^-$ (see Table XIII of [55]). As shown explicitly in Table IV of [55], within the framework of QCDF, the inclusion of $1/m_b$ power corrections to penguin annihilation is responsible for the sign flip of $\mathcal{A}_{CP}(\rho^0\pi^-)$ to a negative one. Specifically, we shall use

$$\beta_3^p[\pi\rho] = -0.03 + 0.02i,$$
$$\beta_3^p[\rho\pi] = 0.004 - 0.049i, \tag{3.17}$$

for $p = u, c$. While the tree-dominated $B^- \to \rho^0\pi^-$ rate is affected only slightly by the power correction, CP asymmetry flips the sign and becomes -0.21. From Table VIII, we see that the inclusive and regional CP asymmetries induced by resonances now become negative. Consequently, the predicted $\mathcal{A}_{CP}^{\rm incl}$ is wrong in sign, while $\mathcal{A}_{CP}^{\rm low}$ and $\mathcal{A}_{CP}^{\rm resc}$ are too small when compared with experiment. Hence, the LHCb data imply positive CP violation induced by the ρ and f_0 resonances. Indeed, LHCb has measured asymmetries in $B^- \to \pi^+\pi^-\pi^-$ in four distinct regions dominated by the ρ [8]: I: $0.47 < m(\pi^+\pi^-)_{\rm low} < 0.77\,{\rm GeV}, \cos\theta > 0$, II: $0.77 < m(\pi^+\pi^-)_{\rm low} < 0.92\,{\rm GeV}, \cos\theta > 0$, III: $0.47 < m(\pi^+\pi^-)_{\rm low} < 0.77$ GeV, $\cos\theta < 0$, and IV: $0.77 < m(\pi^+\pi^-)_{\rm low} < 0.92$ GeV, $\cos\theta < 0$. It is seen that $\mathcal{A}_{CP}$ changes sign at

TABLE VIII. Predicted inclusive and regional CP asymmetries (in %) in $B^- \to \pi^+\pi^-\pi^-$ decay when penguin annihilation is added to render $\mathcal{A}_{CP}(\rho^0\pi^-) \approx -0.21$.

	NR	RES	NR + RES	Expt.
$\mathcal{A}_{CP}^{\rm incl}$	$25.0^{+4.4+2.1+0.0}_{-2.7-3.1-0.1}$	$-16.3^{+0.0+1.5+0.0}_{-0.0-1.0-0.0}$	$-6.7^{+1.6+1.5+0.0}_{-2.6-1.3-0.0}$	5.8 ± 2.4
$\mathcal{A}_{CP}^{\rm low}$	$58.3^{+3.6+2.6+0.8}_{-3.7-4.0-0.8}$	$-16.8^{+0.0+1.5+0.0}_{-0.0-1.1-0.0}$	$6.0^{+0.2+3.1+0.0}_{-0.4-1.2-0.0}$	58.4 ± 9.7
$\mathcal{A}_{CP}^{\rm resc}$	$36.7^{+6.2+3.2+0.1}_{-3.7-4.6-0.2}$	$-11.4^{+0.0+1.5+0.0}_{-0.0-1.0-0.0}$	$0.4^{+1.2+2.0+0.0}_{-2.1-1.8-0.0}$	17.2 ± 2.7

$m(\pi^+\pi^-) \sim m_\rho$. Summing over the regions I–IV yields CP asymmetry consistent with zero with slightly positive central value (see Table IV of [8]).

Therefore, we encounter a puzzle here. On one hand, *BABAR* and LHCb measurements of $B^- \to \pi^+\pi^-\pi^-$ seem to indicate a positive CP asymmetry in the $m(\pi^+\pi^-)$ region peaked at m_ρ. On the other hand, all theories predict a large and negative CP violation in $B^- \to \rho^0\pi^-$. This issue concerning $\mathcal{A}_{CP}(\rho^0\pi^-)$ needs to be resolved.

5. Local CP violation in other invariant mass regions

For regional CP violation, so far we have focused on the small invariant mass region specified in Eq. (1.1) and the rescattering region of $m_{\pi\pi}$ and $m_{K\bar{K}}$ between 1.0 and 1.5 GeV. As noticed in passing, the magnitude and sign of CP asymmetries in the Dalitz plot vary from region to region. A successful model must explain not only the inclusive asymmetry but also regional CP violation. Therefore, the measured CP-asymmetry Dalitz distributions put stringent constraints on the models. In the following, we consider the distribution of $\mathcal{A}_{CP}$ in some (large) invariant mass regions to test our model.

$\underline{B^\pm \to K^\pm K^+ K^-}$

We see from Fig. 3(a) that $\mathcal{A}_{CP}$ is mostly negative in the Dalitz plot region with $m(K^+K^-)_{\rm low}$ between 1 and 1.6 GeV and $m(K^+K^-)_{\rm high}$ below 4 GeV, but it can be positive at $m(K^+K^-)_{\rm high} > 4$ GeV (see also Fig. 2 of [11]). We consider two regions with positive $\mathcal{A}_{CP}$: (i) $m^2(K^+K^-)_{\rm low} = 3$–$5$ GeV^2 and $m^2(K^+K^-)_{\rm high} = 18$–$22$ GeV^2, and (ii) $m^2(K^+K^-)_{\rm low} = 8$–$9$ GeV^2 and $m^2(K^+K^-)_{\rm high} = 18$–$19$ GeV^2. We obtain the values of $\mathcal{A}_{CP}$ to be 0.11 and 0.41, respectively, in our model. This is consistent with the data as $\mathcal{A}_{CP}$ in region (ii) should be much larger than that in region (i).

$\underline{B^\pm \to K^\pm \pi^+ \pi^-}$

While the integrated $\mathcal{A}_{CP}^{\rm incl}$ is positive in this decay, Fig. 3(b) shows the distribution of negative CP asymmetry in the regions such as (i) $m^2(\pi^+\pi^-) = 9.5$–10.5 GeV^2 and $m^2(K^+\pi^-) = 10$–18 GeV^2 and (ii) $m^2(\pi^+\pi^-) = 2$–6 GeV^2 and $m^2(K^+\pi^-) = 20.5$–21.5 GeV^2. Our model leads to $\mathcal{A}_{CP}^{\rm local} \approx -0.09$ and -0.04, respectively. Experimentally, $|\mathcal{A}_{CP}|$ in region (ii) should be larger. Therefore, while the sign is correctly predicted, the relative magnitude of $\mathcal{A}_{CP}$ in regions (i) and (ii) is not borne out by experiment.

$\underline{B^\pm \to \pi^\pm \pi^+ \pi^-}$

It is obvious from Fig. 3(c) that $\mathcal{A}_{CP}$ is very large and positive in the region of $5 < m^2(\pi^+\pi^-)_{\rm low} < 10$ GeV^2 and $9 < m^2(\pi^+\pi^-)_{\rm high} < 12$ GeV^2, and it becomes negative in the region of $3 < m^2(\pi^+\pi^-)_{\rm low} < 8$ GeV^2 and $20 < m^2(\pi^+\pi^-)_{\rm high} < 21$ GeV^2. We obtain $\mathcal{A}_{CP}^{\rm local} \approx 0.47$ and -0.29, respectively, in qualitative agreement with experiment.

$\underline{B^\pm \to \pi^\pm K^+ K^-}$

Figure 3(d) shows that $\mathcal{A}_{CP}$ is large and negative in the region of (i) $16 < m^2(K^+K^-) < 25$ GeV^2 and $5 < m^2(K^+\pi^-) < 10$ GeV^2. It changes sign in the region of (ii) $5 < m^2(K^+K^-) < 9$ GeV^2 and $4 < m^2(K^+\pi^-) < 13$ GeV^2. Our results $\mathcal{A}_{CP}^{\rm local} \approx 0.36$ and -0.44 in regions (i) and (ii), respectively, are not consistent with experiment. If the phase δ is set to zero, we will have $\mathcal{A}_{CP}^{\rm local} \approx -0.73$ and 0.54, respectively, in qualitative agreement with the data. Thus, it is possible that the phase δ is energy dependent, and it vanishes in the large invariant mass region. This issue is currently under study.

In short, for local CP asymmetries in various (large) invariant mass regions, our model predictions are in qualitative agreement with experiment for $K^+K^-K^-$ and $\pi^+\pi^-\pi^-$ modes and yield a correct sign for $K^-\pi^+\pi^-$. However, it appears that the phase δ needs to vanish in the large invariant mass region for $K^+K^-\pi^-$ in order to accommodate the observation.

IV. COMPARISON WITH OTHER WORKS

CP violation in three-body decays of the charged B meson has been investigated in Refs. [5,16–27,66]. The authors of [16,18] considered the possibility of having a large local CP violation in $B^- \to \pi^+\pi^-\pi^-$ resulting from the interference of the resonances $f_0(500)$ and $\rho^0(770)$. A similar mechanism has been applied to the decay $B^- \to K^-\pi^+\pi^-$ [66]. Studies of flavor SU(3) symmetry imposed on the decay amplitudes and its implication on CP violation were elaborated on in [19,23]. The observed CP asymmetry in $B^- \to \pi^+\pi^-\pi^-$ decays changes sign at a value of $m(\pi^+\pi^-)_{\rm low}$ close to the $\rho(770)$ resonance [8]. It was argued in [22] that the sign change is caused by the ρ–ω mixing. In our work, we have taken into account both resonant and nonresonant amplitudes simultaneously and worked out their

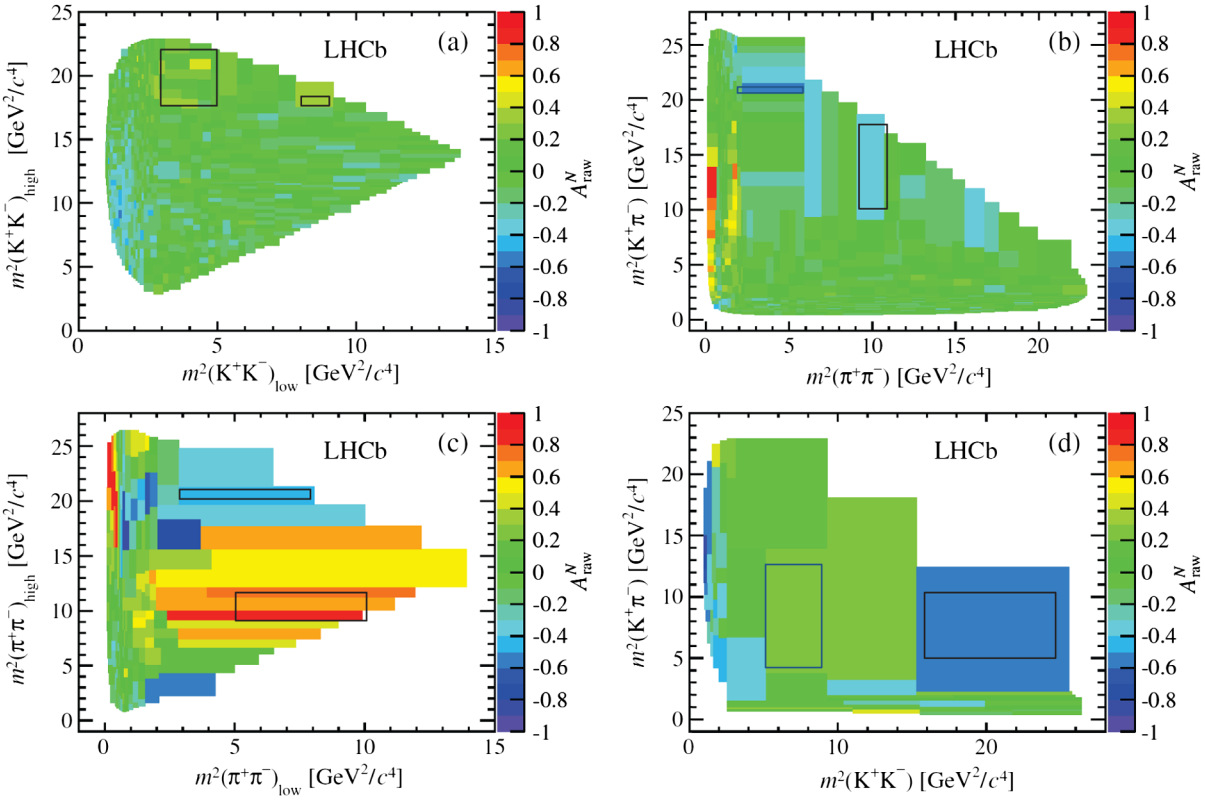

FIG. 3. Local *CP* asymmetry distributions in the invariant mass regions depicted by the black rectangles for (a) $B^\pm \to K^\pm K^+ K^-$, (b) $B^\pm \to K^\pm \pi^+ \pi^-$, (c) $B^\pm \to \pi^\pm \pi^+ \pi^-$, and (d) $B^\pm \to \pi^\pm K^+ K^-$. Dalitz plots of *CP* -asymmetry distributions are taken from [8].

contributions to branching fractions and *CP* violation in details. We found that even in the absence of $f_0(500)$ resonance, local *CP* asymmetry in $\pi^+\pi^-\pi^-$ can already reach the level of 17% due to nonresonant and other resonant contributions. Moreover, the regional asymmetry induced solely by the nonresonant component can be as large as 58% in our calculation. In our work and also in the work of [17,26] to be discussed below, the sign change is ascribed to the real part of the Breit-Wigner propagator for the $\rho(770)$ resonance.

Based on the constraint of *CPT* invariance on final-state interactions, the authors of [17,26] have studied *CP* violation in charmless three-body charged B decays, especially the *CP*-asymmetry distribution in the mass region below 1.6 GeV. We first recapitulate the main points of this work. Writing the S matrix as $S_{\lambda'\lambda} = \delta_{\lambda'\lambda} + it_{\lambda'\lambda}$ and the decay amplitude to the leading order in t as

$$\mathcal{A}(h \to \lambda) = A_\lambda + e^{-i\gamma} B_\lambda + i \sum_{\lambda'} t_{\lambda'\lambda} (A_{\lambda'} + e^{-i\gamma} B_{\lambda'}), \quad (4.1)$$

with A_λ and B_λ being complex amplitudes invariant under *CP*, it follows that the rate difference reads [17,26]

$$\begin{aligned} \Delta\Gamma_\lambda &\equiv \Gamma(h \to \lambda) - \Gamma(\bar{h} \to \bar{\lambda}) \\ &= 4(\sin\gamma)\mathrm{Im}(B_\lambda^* A_\lambda) \\ &\quad + 4(\sin\gamma) \sum_{\lambda'} \mathrm{Re}[B_\lambda^* t_{\lambda'\lambda} A_{\lambda'} - B_{\lambda'}^* t_{\lambda'\lambda}^* A_\lambda] \\ &= \Delta\Gamma_\lambda^{\mathrm{SD}} + \Delta\Gamma_\lambda^{\mathrm{FSI}}, \end{aligned} \quad (4.2)$$

where the first term corresponds to the familiar short-distance contribution to direct *CP* asymmetry and the second term arises from final-state rescattering (so-called compound *CP* violation). It is interesting to notice the relation (see [26] for the derivation)

$$\sum_\lambda \Delta\Gamma_\lambda^{\mathrm{FSI}} = 0 \quad (4.3)$$

is valid irrespective of the short-distance one. When the *CPT* condition $\sum_\lambda \mathrm{Im}[B_\lambda^* A_\lambda] = 0$ is imposed, the *CPT* constraint $\sum_\lambda \Delta\Gamma_\lambda = 0$ follows.

Suppose only the two channels $\alpha = \pi^+\pi^- P^-$ and $\beta = K^+K^- P^-$ ($P = \pi$, K) in B^- decays are strongly coupled through strong interactions with the third meson P being treated as a bachelor or a spectator, it follows from Eq. (4.3) that $\Delta\Gamma_\alpha^{\mathrm{FSI}} = -\Delta\Gamma_\beta^{\mathrm{FSI}}$ (not $\Delta\Gamma_\alpha = -\Delta\Gamma_\beta$!). It should be stressed again that this relation is not imposed by hand, rather it is a consequence of the assumption of only two

channels coupled through final-state resacttering. As a result,

$$\left(\frac{\mathcal{A}_{CP}^{\rm incl}(K^+K^-\pi^-)}{\mathcal{A}_{CP}^{\rm incl}(\pi^+\pi^-\pi^-)}\right)^{\rm FSI} = -\frac{\mathcal{B}(B^-\to\pi^+\pi^-\pi^-)}{\mathcal{B}(B^-\to K^+K^-\pi^-)} = -3.0\pm 0.5,$$
$$\left(\frac{\mathcal{A}_{CP}^{\rm incl}(K^+K^-K^-)}{\mathcal{A}_{CP}^{\rm incl}(\pi^+\pi^-K^-)}\right)^{\rm FSI} = -\frac{\mathcal{B}(B^-\to K^+K^-K^-)}{\mathcal{B}(B^-\to\pi^+\pi^-K^-)} = -1.5\pm 0.1, \quad (4.4)$$

where we have used the branching fractions listed in Table III and the averaged ones: $\mathcal{B}(B^-\to\pi^+\pi^-K^-) = (51.0\pm 2.9)\times 10^{-6}$ and $\mathcal{B}(B^-\to K^+K^-K^-) = (34.0\pm 1.4)\times 10^{-6}$. Experimentally, the ratios in Eq. (4.4) are measured to be of order -2.1 and -1.4, respectively. The coincidence between theory and experiment suggests that the LHCb data of CP asymmetries could be described in terms of final-state rescattering. For three-body B decays, the strong couplings between K^+K^- and $\pi^+\pi^-$ channels with the CPT constraint were used in [26] to fit the observed asymmetries in some channels and then predict CP violation in other modes. Explicitly, the amplitude Eq. (4.1) is fitted to the LHCb data of the distribution of CP asymmetries in $m(\pi^+\pi^-)$ measured in $B^-\to\pi^+\pi^-P^-$ decays with $P=\pi, K$. Then the fit parameters in $\Delta\Gamma_\alpha^{\rm FSI}$ are used to predict the $\Delta\Gamma_\beta^{\rm FSI}(s)$ distributions of $B^-\to K^+K^-P^-$ decays in $m(K^+K^-)$ (see Figs. 10 and 12 of [26]). It turns out that the CP-asymmetry distributions of $B^-\to K^+K^-P^-$ observed by LHCb in the rescattering region are fairly accounted for by the final-state rescattering of $\pi^+\pi^-\leftrightarrow K^+K^-$.

In short, final-state interactions play an essential role in the work of [17,26]. The CPT relation $\Delta\Gamma_\alpha^{\rm FSI} = -\Delta\Gamma_\beta^{\rm FSI}$ is used to describe CP-asymmetry distributions in $B^-\to K^+K^-P^-$ decays after a fit to $B^-\to\pi^+\pi^-P^-$ channels. Final-state rescattering of $\pi^+\pi^-\leftrightarrow K^+K^-$ dominates the asymmetry in the mass region between 1 and 1.5 GeV. On the contrary, we performed a dynamical model calculation of partial rates and CP asymmetries without taking into account final-state interactions explicitly. We accentuate the crucial role played by nonresonant contributions. Our predicted inclusive CP asymmetries for $\pi^+\pi^-\pi^-$ and $K^+K^-K^-$ agree with experiment and have nothing to do with $\pi^+\pi^-$ and K^+K^- final-state rescattering, while the calculated CP asymmetries for $K^+K^-\pi^-$ and $\pi^+\pi^-K^-$ are wrong in sign. Hence, we introduce an additional strong phase δ to flip the sign.

V. CONCLUSIONS

We have presented in this work a study of charmless three-body decays of B mesons using a simple model based on the factorization approach. Our main results are

(i) Dominant nonresonant contributions to tree-dominated and penguin-dominated three-body decays arise from the $b\to u$ tree transition and $b\to s$ penguin transition, respectively. The former can be evaluated in the framework of heavy meson chiral perturbation theory supplemented by some energy dependence to ensure that HMChPT results are valid in a chiral limit. The latter is governed by the matrix element of the scalar density $\langle M_1M_2|\bar q_1 q_2|0\rangle$.

(ii) Based on the factorization approach, we have considered the resonant contributions to three-body decays and computed the rates for the quasi-two-body decays $B\to VP$ and $B\to SP$. While the calculated branching fractions for the tree-dominated modes such as $\rho\pi$ and $f_0(980)\pi$ are consistent with experiment, the predicted rates for penguin-dominated $\phi K, K^*\pi, \rho K$, and $K_0^*(1430)\pi$ channels are too small compared to the data. This implies the importance of power corrections. We follow the QCD factorization approach to introduce the penguin annihilation characterized by the parameter β_3 to improve the discrepancy between theory and experiment for penguin-dominated ones.

(iii) The branching fraction of nonresonant contributions is of order $(15\text{–}20)\times 10^{-6}$ in penguin-dominated decays $B^-\to K^+K^-K^-, K^-\pi^+\pi^-$ and of order $(3\text{–}5)\times 10^{-6}$ in tree-dominated decays $B^-\to\pi^+\pi^-\pi^-, K^+K^-\pi^-$. The nonresonant fraction is predicted to be around 55% for the $B^-\to K^+K^-\pi^-$ decay.

(iv) We have updated the predictions for the resonant and nonresonant contributions to $B^-\to\bar K^0\pi^-\pi^0$, $B^-\to K^-\pi^0\pi^0$, $\bar B^0\to\bar K^0\pi^+\pi^-$, and $\bar B^0\to K^-\pi^+\pi^0$. The calculated total branching fractions are smaller than experiment. This is ascribed to the fact that the predicted $B\to K_0^*(1430)\pi$ rates in factorization or QCDF are too small compared to the data and that the $K_0^*(1430)$ has the largest contributions to $B\to K\pi\pi$ decays.

(v) In our study of $B^-\to\pi^-\pi^+\pi^-$, we find that $\mathcal{A}_{CP}(\rho^0\pi^-)$ is positive. Indeed, both *BABAR* and LHCb measurements of $B^-\to\pi^+\pi^-\pi^-$ indicate positive CP asymmetry in the $m(\pi^+\pi^-)$ region peaked at m_ρ. On the other hand, all theories predict a large and negative CP violation in $B^-\to\rho^0\pi^-$. We have shown that if we add $1/m_b$ penguin-annihilation induced power correction to render $\mathcal{A}_{CP}(\rho^0\pi^-)$ negative, $\mathcal{A}_{CP}^{\rm incl}$ will be wrong in sign and the predicted regional CP asymmetries will become too small compared to experiment. Therefore, the issue with CP violation in $B^-\to\rho^0\pi^-$ needs to be resolved.

(vi) While the calculated direct CP asymmetries for $K^+K^-K^-$ and $\pi^+\pi^-\pi^-$ modes are in good agreement with experiment in both magnitude and sign, the predicted asymmetries in $B^-\to\pi^-K^+K^-$ and

$B^- \to K^-\pi^+\pi^-$ are wrong in signs when confronted with experiment. This is attributed to the sizable nonresonant contributions which are opposite in sign to the experimental measurements (see Table VI). We have studied final-state inelastic $\pi^+\pi^- \leftrightarrow K^+K^-$ rescattering and found that CP violation for both $\pi^+\pi^-\pi^-$ and $K^+K^-K^-$ is heading to the wrong direction, making the discrepancy even worse. In order to accommodate the branching fraction of nonresonant component and CP asymmetry observed in $B^- \to K^-\pi^+\pi^-$, the matrix element $\langle K\pi|\bar{s}q|0\rangle$ should have an extra strong phase δ of order $\pm\pi$ in addition to the phase characterized by the parameter $\sigma_{\rm NR}$. This phase δ may arise from some sort of power corrections such as final-state interactions. The matrix element $\langle K\pi|\bar{q}s|0\rangle$ relevant to the decay $B^- \to \pi^-K^+K^-$ is related to $\langle K\pi|\bar{s}q|0\rangle$ via U-spin symmetry.

(vii) In this work, there are three sources of strong phases: effective Wilson coefficients, propagators of resonances, and the matrix element of scalar density $\langle M_1M_2|\bar{q}_1q_2|0\rangle$. There are two sources for the phase in the penguin matrix element of scalar densities: $\sigma_{\rm NR}$ and δ for $K\pi$–vacuum matrix elements.

(viii) Nonresonant CP violation is usually much larger than the resonant one and the interference effect between resonant and nonresonant components is generally quite significant. If nonresonant contributions are turned off in the $B^- \to K^+K^-K^-$ mode, the predicted CP asymmetries due to resonances will be incorrect in sign. Since this decay is predominated by the nonresonant background, the magnitude and the sign of its CP asymmetry should be governed by the nonresonant term.

(ix) We have studied CP-asymmetry Dalitz distributions in some (large) invariant mass regions to test our model. Our model predictions are in qualitative agreement with experiment for $K^+K^-K^-$ and $\pi^+\pi^-\pi^-$ modes and yield a correct sign for $K^-\pi^+\pi^-$. However, it appears that the phase δ needs to vanish in the large invariant mass region for $K^+K^-\pi^-$ in order to accommodate the observation.

ACKNOWLEDGMENTS

This work was supported in part by the Ministry of Science and Technology of Taiwan under Grants No. MOST 104-2112-M-001-022 and No. 103-2112-M-033-002-MY3 and by the National Natural Science Foundation of China under Grant No. 11347030, the Program of Science and Technology Innovation Talents in Universities of Henan Province 14HASTIT037.

[1] K. A. Olive *et al.* (Particle Data Group Collaboration), Chin. Phys. C **38**, 090001 (2014).
[2] Y. Amhis *et al.* (Heavy Flavor Averaging Group Collaboration), arXiv:1412.7515 and online updates at http://www.slac.stanford.edu/xorg/hfag.
[3] J. P. Lees *et al.* (*BABAR* Collaboration), arXiv:1501.00705.
[4] R. Aaij *et al.* (LHCb Collaboration), Phys. Rev. Lett. **110**, 221601 (2013).
[5] H. Y. Cheng and C. K. Chua, Phys. Rev. D **88**, 114014 (2013).
[6] R. Aaij *et al.* (LHCb Collaboration), Phys. Rev. Lett. **111**, 101801 (2013).
[7] R. Aaij *et al.* (LHCb Collaboration), Phys. Rev. Lett. **112**, 011801 (2014).
[8] R. Aaij *et al.* (LHCb Collaboration), Phys. Rev. D **90**, 112004 (2014).
[9] B. Aubert *et al.* (*BABAR* Collaboration), Phys. Rev. D **78**, 012004 (2008).
[10] A. Garmash *et al.* (Belle Collaboration), Phys. Rev. Lett. **96**, 251803 (2006).
[11] R. Aaij *et al.* (LHCb Collaboration), Reports No. CERN-PH-EH-2014-203, No. LHCb-PAPER-2014-044, https://cds.cern.ch/record/1751517?ln=en.
[12] H. Y. Cheng, C. K. Chua, and A. Soni, Phys. Rev. D **76**, 094006 (2007).
[13] T. M. Yan, H. Y. Cheng, C. Y. Cheung, G. L. Lin, Y. C. Lin, and H. L. Yu, Phys. Rev. D **46**, 1148 (1992); **55**, 5851(E) (1997).
[14] M. B. Wise, Phys. Rev. D **45**, R2188 (1992).
[15] G. Burdman and J. F. Donoghue, Phys. Lett. B **280**, 287 (1992).
[16] B. Bhattacharya, M. Gronau, and J. L. Rosner, Phys. Lett. B **726**, 337 (2013).
[17] I. Bediaga, T. Frederico, and O. Lourenco, Phys. Rev. D **89**, 094013 (2014).
[18] Z. H. Zhang, X. H. Guo, and Y. D. Yang, Phys. Rev. D **87**, 076007 (2013).
[19] D. Xu, G. N. Li, and X. G. He, Int. J. Mod. Phys. A **29**, 1450011 (2014); Phys. Lett. B **728**, 579 (2014); X. G. He, G. N. Li, and D. Xu, Phys. Rev. D **91**, 014029 (2015).
[20] L. Leśniak and P. Żenczykowski, Phys. Lett. B **737**, 201 (2014).
[21] Y. Li, Phys. Rev. D **89**, 094007 (2014).
[22] W. F. Wang, H. C. Hu, H. n. Li, and C. D. Lu, Phys. Rev. D **89**, 074031 (2014).
[23] B. Bhattacharya, M. Gronau, M. Imbeault, D. London, and J. L. Rosner, Phys. Rev. D **89**, 074043 (2014).
[24] S. Kräkl, T. Mannel, and J. Virto, Nucl. Phys. **B899**, 247 (2015).

[25] C. Wang, Z. H. Zhang, Z. Y. Wang, and X. H. Guo, Eur. Phys. J. C **75**, 536 (2015).
[26] J. H. A. Nogueira, I. Bediaga, A. B. R. Cavalcante, T. Frederico, and O. Loureno, Phys. Rev. D **92**, 054010 (2015).
[27] I. Bediaga and P. C. Magalhãs, arXiv:1512.09284.
[28] I. Bediaga, in Workshop of Future Challenges in Non-Leptonic B Decays: Theory and Experiment, Bad Honnef, Germany, February 10–12, 2016.
[29] M. Beneke, G. Buchalla, M. Neubert, and C. T. Sachrajda, Phys. Rev. Lett. **83**, 1914 (1999); Nucl. Phys. **B591**, 313 (2000); **B606**, 245 (2001).
[30] Y. Y. Keum, H. n. Li, and A. I. Sanda, Phys. Rev. D **63**, 054008 (2001); Phys. Lett. B **504**, 6 (2001).
[31] C. W. Bauer, S. Fleming, D. Pirjol, and I. W. Stewart, Phys. Rev. D **63**, 114020 (2001).
[32] C. H. Chen and H. n. Li, Phys. Lett. B **561**, 258 (2003).
[33] S. Faller, T. Feldmann, A. Khodjamirian, T. Mannel, and D. van Dyk, Phys. Rev. D **89**, 014015 (2014).
[34] C. Hambrock and A. Khodjamirian, Nucl. Phys. **B905**, 373 (2016).
[35] D. van Dyk, A. Khodjamirian, P. R. Garcés, P. Masiuan, and B. Kubis in Workshop of Future Challenges in Non-Leptonic B Decays: Theory and Experiment, Bad Honnef, Germany, February 10–12, 2016.
[36] J. P. Lees *et al.* (*BABAR* Collaboration), Phys. Rev. D **85**, 112010 (2012).
[37] A. Garmash *et al.* (Belle Collaboration), Phys. Rev. D **71**, 092003 (2005).
[38] J. P. Lees *et al.* (*BABAR* Collaboration), Phys. Rev. D **85**, 054023 (2012).
[39] B. Aubert *et al.* (*BABAR* Collaboration), Phys. Rev. D **80**, 112001 (2009).
[40] A. Garmash *et al.* (Belle Collaboration), Phys. Rev. D **75**, 012006 (2007).
[41] J. P. Lees *et al.* (*BABAR* Collaboration), Phys. Rev. D **83**, 112010 (2011).
[42] P. Chang *et al.* (Belle Collaboration), Phys. Lett. B **599**, 148 (2004).
[43] B. Aubert *et al.* (*BABAR* Collaboration), Phys. Rev. D **79**, 0720106 (2009).
[44] C. L. Y. Lee, M. Lu, and M. B. Wise, Phys. Rev. D **46**, 5040 (1992).
[45] B. Aubert *et al.* (*BABAR* Collaboration), Phys. Rev. D **74**, 032003 (2006); arXiv:0808.0700v2.
[46] B. Aubert *et al.* (*BABAR* Collaboration), Phys. Rev. Lett. **99**, 221801 (2007).
[47] A. Garmash *et al.* (Belle Collaboration), Phys. Rev. D **69**, 012001 (2004).
[48] See Chapter 13 of A. J. Bevan *et al.* (*BABAR* and Belle Collaborations), Eur. Phys. J. C **74**, 3026 (2014).
[49] S. M. Flatté, Phys. Lett. **63B**, 224 (1976).
[50] C. K. Chua, W. S. Hou, S. Y. Shiau, and S. Y. Tsai, Phys. Rev. D **67**, 034012 (2003).
[51] M. Doring, U. G. Meisner, and W. Wang, J. High Energy Phys. 10 (2013) 011; U. G. Meisner and W. Wang, Phys. Lett. B **730**, 336 (2014).
[52] B. Aubert *et al.* (*BABAR* Collaboration), Phys. Rev. Lett. **99**, 161802 (2007).
[53] J. Charles, A. Höcker, H. Lacker, S. Laplace, F. R. Diberder, J. Malclés, J. Ocariz, M. Pivk, and L. Roos (CKMfitter Group), Eur. Phys. J. C **41**, 1 (2005) and updated results from http://ckmfitter.in2p3.fr; M. Bona *et al.* (UTfit Collaboration), J. High Energy Phys. 07 (2005) 028 and updated results from http://utfit.roma1.infn.it.
[54] M. Beneke and M. Neubert, Nucl. Phys. **B675**, 333 (2003).
[55] H. Y. Cheng and C. K. Chua, Phys. Rev. D **80**, 114008 (2009).
[56] H. Y. Cheng, C. K. Chua, K. C. Yang, and Z. Q. Zhang, Phys. Rev. D **87**, 114001 (2013).
[57] H. Y. Cheng, C. K. Chua, and K. C. Yang, Phys. Rev. D **73**, 014017 (2006).
[58] J. P. Lees *et al.* (*BABAR* Collaboration), Phys. Rev. D **84**, 092007 (2011).
[59] I. I. Bigi, arXiv:1306.6014; arXiv:1509.03899.
[60] D. Atwood and A. Soni, Phys. Rev. D **58**, 036005 (1998).
[61] M. Bander, D. Silverman, and A. Soni, Phys. Rev. Lett. **43**, 242 (1979).
[62] H. Y. Cheng, C. K. Chua, and A. Soni, Phys. Rev. D **71**, 014030 (2005).
[63] J. R. Pelaez and F. J. Yndurain, Phys. Rev. D **71**, 074016 (2005).
[64] C. K. Chua, Phys. Rev. D **78**, 076002 (2008).
[65] M. Suzuki and L. Wolfenstein, Phys. Rev. D **60**, 074019 (1999).
[66] Z. H. Zhang, X. H. Guo, and Y. D. Yang, arXiv:1308.5242.